Financial Uncertainty with Ambiguity and Learning

DOI:
10.1287/mnsc.2021.3958

Document Version
Accepted author manuscript

Financial Uncertainty with Ambiguity and Learning

Hening Liu*

Alliance Manchester Business School
The University of Manchester

Yuzhao Zhang†‡

Rutgers Business School
Rutgers University

September, 2020

Abstract

We examine a production-based asset pricing model with regime-switching productivity growth, learning and ambiguity. Both mean and volatility of the growth rate of productivity are assumed to follow a Markov chain with an unobservable state. The agent's preferences are characterized by the generalized recursive smooth ambiguity utility function. Our calibrated benchmark model with modest risk aversion can match moments of the variance risk premium in the data and reconcile empirical relations between the risk-neutral variance and macroeconomic quantities and their volatilities respectively. We show that the interplay between productivity volatility risk and ambiguity aversion is important for pricing variance risk in returns.

JEL Classification: C61; D81; G11; G12.

Keywords: Ambiguity, business cycle, Markov switching, production-based asset pricing, uncertainty, variance risk premium.

*Alliance Manchester Business School, The University of Manchester, Booth Street West, Manchester M15 6PB, UK. e-mail: hening.liu@manchester.ac.uk.

†Rutgers Business School, Rutgers, The State University of New Jersey; Newark, NJ, 07102, USA. e-mail: yzhang@business.rutgers.edu.

‡We thank Tomasz Piskorski (the editor), an associate editor, and two anonymous referees for many useful comments. We also thank Daniele Bianchi, Michael Brennan, Jie Cao, Ilan Cooper, Max Croce, Andras Fulop, Cosmin Ilut, Junye Li, Jianjun Miao, Mohammad Jahan-Parvar, Roman Sustek, Maxim Ulrich and seminar participants at SAFE Asset Pricing Workshop (Frankfurt), International Conference on Computational and Financial Econometrics (2015), BI Norwegian Business School, ESSEC Business School, Queen Mary University of London, the Chinese University of Hong Kong, University of Essex and Warwick Business School for helpful comments. This paper was previously circulated under the title "Ambiguity and financial uncertainty in a real business cycle model." All errors are our own.

1 Introduction

Financial uncertainty has drawn growing attention in recent macro-finance research. The most common measure of financial uncertainty is the Chicago Board Options Exchange's volatility index (VIX). VIX measures how much investors are willing to pay for S&P 500 index options and gauges investors' fear of economic uncertainty under the risk-neutral measure. To hedge against investors' fear of uncertainty, investors pay a premium to buy equity index options, which results in the variance risk premium (VRP), defined as the difference between the expected stock return variances under the risk-neutral and physical measures. Both the average and standard deviation of the variance risk premium are large and cannot be explained by standard asset pricing models, leading to the "variance risk premium puzzle". The empirical distribution of the variance risk premium is also non-normal, with a positive skewness and high kurtosis. Empirically, spikes in VIX and VRP tend to coincide with times of high economic uncertainty, which subsequently leads to economic downturns. Some studies have interpreted this observation as suggesting that uncertainty shocks may be an important driver of business cycles. Bloom (2009) and Bloom et al. (2018) build general equilibrium models in which uncertainty shocks drive business cycles.

In this paper, we examine a production-based, representative-agent asset pricing model in which the growth rate of productivity follows a regime-switching process and the agent is ambiguity averse. In the model, the dynamics of conditional mean and volatility of productivity growth are characterized by a Markov chain. Our model selection procedure suggests the choice of a three-regime model that identifies three regimes as 1) high mean and low volatility (good) regime, 2) normal mean and medium volatility (normal) regime, and 3) low mean and high volatility (bad) regime. Empirical estimates of the transition probabilities indicate that all the regimes exhibit persistence and that none of them is an absorbing state.

Previous literature has revealed the importance of ambiguity for studying asset prices, see Chen and Epstein (2002), Anderson, Hansen, and Sargent (2003), Ju and Miao (2012), among others. To embed the agent's ambiguity attitude in the model, we follow Jahan-Parvar and Liu (2014) and assume that the agent cannot observe the underlying state of the productivity growth process but can learn about the state via Bayes' rule. Ambiguity arises due to uncertainty faced by the agent in estimating mean and volatility of productivity growth that depend on the state of the

economy. The agent learns about the volatility state because it cannot simply be observed through high frequency data. Furthermore, we assume that the agent is ambiguity averse in the spirit of Hayashi and Miao (2011) and Klibanoff, Marinacci, and Mukerji (2005, 2009) and that the agent's preferences are represented by the generalized recursive smooth ambiguity utility function proposed by Ju and Miao (2012) and Hayashi and Miao (2011). These two papers show that the pricing kernel under the generalized smooth ambiguity preferences implies endogenous pessimism. In a comprehensive study on structural estimation of asset pricing models, Gallant et al. (2019) demonstrate that incorporating ambiguity aversion is important for obtaining reasonable estimates of risk aversion.

We calibrate the model to match empirical regularities of macroeconomic quantities including smooth consumption growth, volatile investment growth and comovement among consumption, investment and output. With moderate risk aversion and an elasticity of intertemporal substitution (EIS) greater than 1, our benchmark model with ambiguity aversion generates a low and smooth risk-free rate and a high equity premium. Remarkably, the model can also match the mean, volatility, skewness and kurtosis of variance risk premium in the data. We also price call and put options with different maturities (1 to 4 quarters) across a wide range of moneyness using simulations and find that the benchmark model generates an implied volatility skew, consistent with the empirical regularities in the data. The implied volatility monotonically decreases with the strike price. Furthermore, the benchmark model matches the implied volatility in the data well, especially for low strike out-of-the-money put options, for all maturities. One limitation, though, is that the model generated time series of the risk-neutral variance and the variance risk premium only moderately correlate with the historical data series.

Our model can reproduce the negative impacts of a rise in VIX on quantities that have been documented extensively in empirical literature. In fact, this result can be endogenously generated from our model when the economy experiences severe shocks to productivity. Because the agent's belief about productivity states deteriorates, quantities including investment, consumption and hours worked decline while the heightened uncertainty in presence of ambiguity aversion substantially raises the price of volatility risk and variance risk premium as a result. These results clearly indicate that the endogenous pessimism due to ambiguity aversion is important for pricing

volatility risk in returns. Apart from that, the endogenous pessimism greatly decreases the equity value but increases conditional equity premium. Thus, in line with existing empirical results (see Bollerslev, Tauchen, and Zhou (2009), Bali and Zhou (2016) and Zhou (2018)), the risk-neutral variance carries a positive risk premium in our model.

The analysis of pricing variance risk in equilibrium settings has so far been confined to endowment economies, for example, see Bollerslev et al. (2009), Drechsler and Yaron (2011), Drechsler (2013), Zhou and Zhu (2014), Zhou (2018), and Miao, Wei, and Zhou (2018). These studies primarily rely on elements such as stochastic volatility of volatility, jump risks and model misspecification in long run risk environments. In these models, consumption volatility and the model-implied VIX are close to perfectly correlated by construction. To distinguish the two types of uncertainty, it is useful to consider production economies by which we can study the joint behavior of business cycles and asset prices. The model-implied correlation between volatilities of quantities and the model-implied VIX is far less than the correlation in endowment economies. Consumption-based models are also silent on the relations between VIX and other macroeconomic variables, whereas our model provides theoretical predictions on these relations.

Two closely related papers to ours include Miao et al. (2018) and Jahan-Parvar and Liu (2014). Miao et al. (2018) employ the smooth ambiguity model to examine variance risk premium in the consumption-based framework. Jahan-Parvar and Liu (2014) also use the same utility function as in this paper to investigate implications of ambiguity on quantities and asset returns in a real business cycle (RBC) model. Our analysis differs from them in important aspects. First, our model features time-varying volatility whereas constant volatility is assumed in both Miao et al. (2018) and Jahan-Parvar and Liu (2014). We show that regime-switching volatility in productivity growth and the associated ambiguity about volatility regimes are important for producing significant volatility risk in returns and for pricing volatility risk. In a model comparison exercise, we show that in absence of time-varying productivity volatility, the mean and volatility of VRP are close to 0, and its skewness and kurtosis are inconsistent with the data.

Second, time-varying productivity volatility is an important ingredient for reconciling the empirical lead-lag relations between VIX and volatilities of quantities observed in the data. The empirical analysis shows that VIX leads macroeconomic uncertainty positively, which is consistent

with the prediction of our benchmark model. Without productivity volatility risk, the model is unable to generate a significantly positive relation between VIX and consumption volatility, which is, nevertheless, an important empirical observation and at the heart of a number of consumption-based models (e.g., Bollerslev et al. (2009), Drechsler (2013), Zhou and Zhu (2014) and Bali and Zhou (2016)).

Third, different from previous asset pricing models with learning in which a two-state Markov-switching process is commonly employed (e.g., David (1997), Veronesi (1999), Cagetti, Hansen, Sargent, and Williams (2002), Cogley and Sargent (2008), Ju and Miao (2012), Miao et al. (2018) and Jahan-Parvar and Liu (2014)), our benchmark model has three regimes for productivity growth and the agent must update his belief about all the regimes. Uncertainty represented by fluctuating beliefs is priced in our model. This feature also distinguish our study from Johannes, Lochstoer, and Mou (2016) in which the anticipated utility approach is adopted and thus future uncertainty is not priced. Our choice of the three-regime model is guided not only on the ground of empirical estimation but also model calibration. Quantitative analysis shows that the benchmark model with three regimes can match moments of the equity premium and the VRP better than an alternative model with two regimes does. In particular, the two-regime model that matches the mean equity premium produces a very low VRP.[1]

Our main asset pricing results presented in the paper are based on pricing exogenous market dividends rather than on endogenous firms' payouts implied in a RBC model. In a typical RBC model, during high productivity growth periods, investments are high and the payouts consequently tend to be low. As such, payouts are countercyclical and most risk in the equity claim is removed, leading to counterfactually low equity volatility and equity premium.[2] In addition, the return on investment has low risks because the capital stock is a slow-moving state variable. For these reasons, we follow the consumption-based asset pricing literature (Abel (1999), Bansal and Yaron (2004) and Ju and Miao (2012), among others) to assume that aggregate dividends are a levered claim on aggregate consumption. Thus, dividends become procyclical, consistent with the data. Moreover, our model also implies that the dividend volatility positively forecasts the equity premium, which

[1]For the sake of brevity, these results are not shown in the paper but can be found in the Internet Appendix.

[2]Favilukis and Lin (2015) and Kuehn et al. (2013) introduce labor market frictions in RBC models and show that the models can generate procyclical variation in firms' payouts. Examining the interaction of ambiguity and labor market frictions in a production economy with heterogeneous firms is beyond our scope and left for future research.

is consistent with the findings of Li and Yang (2013). In fact, we have also done the analysis based on endogenous firms' payout. We follow Jermann (1998) to introduce financial leverage in our model. We find that for this model the relations among productivity risks, VIX, quantities and their volatilities and other financial variables are similar to the benchmark model with exogenous market dividends except that the model with financial leverage still cannot match the equity premium, the volatility of returns, and the VRP. These results are reported in the Internet Appendix.

This paper is also connected to the production-based asset pricing literature and asset pricing under ambiguity. Ai (2010) analyze information quality in a long-run risk model and the associated welfare implication. Kaltenbrunner and Lochstoer (2010) study implications of recursive preferences on quantities and asset returns in RBC models with autoregressive productivity levels and i.i.d. productivity growth. Croce (2014) first introduces long-run productivity risk and finds that the model can match salient features of quantities and asset returns well. Gourio (2012) examines the impacts of time-varying disaster risk on business cycles and asset prices. Liu and Miao (2015) study generalized disappointment aversion and volatility risk. But these studies do not consider the interaction of learning and smooth ambiguity. Similar to our paper, Backus, Ferriere, and Zin (2015) and Altug et al. (2020) investigate smooth ambiguity preferences in production economies. They do not examine financial uncertainty in the context of learning, which, however, is our focus. Ilut and Schneider (2014) and Bianchi, Ilut, and Schneider (2018) estimate dynamic stochastic general equilibrium models with ambiguity and examine its implications on asset prices. Both studies adopt multiple priors to model ambiguity. They do not consider recursive preferences in their analysis. Neither do they examine financial uncertainty.

The rest of our paper is organized as follows. Section 2 provides empirical analysis on the econometric specification of productivity growth and the impact of risk-neutral variance on quantities and asset prices. Section 3 presents a model with smooth ambiguity preferences and Markov switching productivity growth rates. Section 4 calibrates the model to the historical data, discusses quantitative results, and performs model comparison. Section 5 concludes this paper. The numerical algorithm, methods of calibrating ambiguity aversion and additional calibration and simulation results are described in the Internet Appendix.

2 Empirical Analysis

2.1 Risk-neutral variance and variance risk premium

The market variance risk premium is not directly observable, but can be estimated from the difference between the model-free implied variance and the conditional expectation of realized variance. Formally, the variance risk premium is defined as the difference between the return variance under the risk-measure and that under the objective measure,

$$VRP_t \equiv \mathrm{Var}_t^Q \left[r_{t+1} \right] - \mathrm{Var}_t \left[r_{t+1} \right],$$

for which $\mathrm{Var}_t^Q [\cdot]$ denotes the risk-neutral variance, $\mathrm{Var}_t [\cdot]$ is variance under the physical expectation.

We compute the risk-neutral variance $\mathrm{Var}_t^Q [r_{t+1}]$ following the volatility index (VIX) method used by the Chicago Board of Options Exchange (CBOE), and therfore denote the computed risk-neutral variance VIX^2,

$$VIX_t^2 = \frac{2}{T} \sum_i \frac{\Delta X_i}{X_i^2} e^{r_f T} Q(X_i, T) - \frac{1}{T} \left[\frac{F}{X_0} - 1 \right]^2,$$

for which T is time to maturity, X_i is the strike price of the ith out-of-the-money option, r_f is the LIBOR rate for maturity T, $Q(X_i, T)$ is the midpoint of bid and ask prices for option with maturity T and strike X_i, F is the forward index level derived from the put-call parity using index option prices, and X_0 is the first strike below F. The LIBOR yield curve, S&P500 index returns, and options data for the period between January 1996 to April 2016 are from OptionMetrics. For the sample period between January 1990 to December 1996, the LIBOR yield curve and S&P500 index (SPX) returns are from Global Financial Data (GFD) and options data are from Market Data Express. Overall, our sample of VIX data spans from January 1990 to April 2016. Because real business cycle models are often calibrated at quarterly frequencies, we construct quarterly market risk-neutral variance and variance risk premium data at every quarter end. In particular, we compute the risk-neutral variance with SPX index option prices for the maturity on either side of 90 days and linearly interpolate the risk-neutral variance to obtain the 90-day constant maturity,

risk-neutral variance.

The objective variance, VOL_t^2, is estimated from daily S&P500 index (SPX) log returns, to be consistent with the VIX computation. To estimate the quarterly variance under the physical measure, we first compute the sum of squared daily log returns of the quarter leading up to time t,

$$RV_t = \sum_{j=0}^{T} r_{t-j}^2.$$

We sample returns daily because they correspond to the most common measurement frequency used in variance trading instruments (i.e. variance swaps). Then we regress RV_{t+1} on its on its own lag, RV_t, and lagged risk-neutral variance, VIX_t^2, and use fitted value as conditional variance under the physical measure, denoted as VOL_t^2. We follow Drechsler and Yaron (2011) and Drechsler (2013) in forming the conditional variance using this approach[3] and the variance risk premium is therefore computed as $VIX_t^2 - VOL_t^2$.

2.2 Markov-switching models and the VAR analysis

Several papers have analyzed the impact of uncertainty shocks on the business cycle. This literature considers different measures of uncertainty, including the VIX measure (Bloom (2009)), the dispersion of total factor productivity (TFP) shocks to plants and establishments (Bloom et al. (2018)), survey data (Leduc and Liu (2016)), and the time-varying volatility of TFP growth (Liu and Miao (2015)). All of these studies find that an increase in uncertainty dampens real economic activity. Accordingly, we want to empirically examine the link between time-varying volatility of productivity growth and the risk-neutral variance that is used as a proxy for financial uncertainty. In addition, our empirical analysis reproduces results in previous studies that financial uncertainty has negative impacts on aggregate quantities. We then rely on our empirical analysis to motivate several production-based models in the next section.

We denote by Δa_t the productivity growth rate, $\Delta a_t \equiv \ln(A_t/A_{t-1})$ for which A_t is the pro-

[3] Alternatively, we also compute the physical conditional variance by simply using last calendar quarter's realized variance and the resulting variance risk premium are very similar. For robustness, daily simple returns are also used in place of daily log returns and the results are quantitatively almost identical. These robustness results are available upon request.

ductivity level. We assume that productivity growth follows a Markov switching (MS) process,

$$\Delta a_t = \mu(s_t) + \sigma(s_t)\,\epsilon_t, \quad \epsilon_t \sim N(0,1), \tag{1}$$

for which s_t determines the regime of the conditional mean and volatility of the growth rate and s_t evolves according to a Markov chain. Previous studies have extensively investigated MS models and asset prices in consumption- and production-based equilibrium frameworks, see David (1997), Veronesi (1999), Cecchetti, Lam, and Mark (2000), Cagetti et al. (2002), Cogley and Sargent (2008) and Johannes et al. (2016), among others. We denote by $\boldsymbol{P}$ the transition matrix of the Markov chain and $\boldsymbol{\pi}_t$ the posterior belief vector about the next period's states. The transition probability p_{ij} in matrix $\boldsymbol{P}$ is defined as $p_{ij} = \Pr(s_t = j | s_{t-1} = i)$. Given the prior belief vector $\boldsymbol{\pi}_0$ and according to Bayes' rule, the posterior belief $\boldsymbol{\pi}_t$ is given by

$$\boldsymbol{\pi}_t = \boldsymbol{P}' \frac{\boldsymbol{\pi}_{t-1} \odot \boldsymbol{f}_t}{\mathbf{1}'(\boldsymbol{\pi}_{t-1} \odot \boldsymbol{f}_t)}, \tag{2}$$

where f_t is a vector of conditional Gaussian likelihood functions for $\mu(s_t)$ and $\sigma(s_t)$, $\odot$ denotes element-wise multiplication, and $\mathbf{1}$ is a vector of ones.

We use macroeconomic data to construct Solow residuals and quarterly productivity growth rates. The sample period for empirical estimation of the MS models is 1947:Q1—2016:Q1. Details of data construction are included in the Internet Appendix. We estimate two-regime, three-regime and four regime MS models using the expectation maximization algorithm developed by Hamilton (1990). The parameter estimates for the two-regime and three-regime models are summarized in Table 1.[4] For all the MS models that we consider, we find that imposing the restriction of constant volatility results in significant underperformance in terms of the likelihood and Bayesian Information Criteria (BIC).

Our estimation results for the two-regime MS model are presented in Panel A of Table 1. Two distinct regimes are identified for which the expansion regime is characterized by high mean growth and low volatility and the contraction regime by low mean growth and high volatility. In

[4]Based on criteria including the likelihood and Bayesian Information Criteria (BIC), the four-regime model is the least preferred model and thus omitted in the analysis below. Moreover, we have encountered the curse of dimensionality in solving model equilibrium with the four-regime MS model and learning.

the contraction regime, the mean growth rate of productivity is negative and the volatility is three times higher than that in the expansion regime The estimates of the transition probabilities indicate that the expansion regime is more persistent than the contraction regime. All of our estimates are statistically significant. These results are similar to those reported in previous studies such as Cagetti et al. (2002), Cogley and Sargent (2008) and Johannes et al. (2016).

The estimation results for the three-regime MS model are presented in Panel B of Table 1. These estimates reveal three different regimes. They are 1) high mean and low volatility (good) regime ($\mu_3 = 1.967$, $\sigma_3 = 0.597$), 2) normal mean and medium volatility (normal) regime ($\mu_2 = 0.821$, $\sigma_2 = 1.021$), and 3) low mean and high volatility (bad) regime ($\mu_1 = -0.61$, $\sigma_1 = 3.674$). The estimates of the transition probabilities p_{11}, p_{22} and p_{33} show that all of the three regimes exhibit persistence, with the normal regime having the highest level of persistence. Model selection based on the log likelihood and BIC suggests that the three-regime model is preferred to the two-regime model even though the three-regime model has many more parameters.

[Insert Table 1 about here]

We ask the question: does an increase in the conditional volatility of productivity growth lead to more financial uncertainty as proxied by the risk-neutral variance, which subsequently causes declines in the macroeconomic quantities and equity valuation? To answer this question, we perform a Vector Autoregressive (VAR) analysis with six endogenous variables, including conditional volatility of productivity growth, risk-neutral variance, consumption, investment, hours worked, and the price-dividend ratio. All variables are expressed in logarithms. Macroeconomic data are drawn from the National Income and Product Accounts (NIPA). Consumption and investment data are deflated by the corresponding deflators. The price-dividend ratio data are constructed from value-weighted index returns that include and exclude distributions. Stock returns data are drawn from the Center for Research in Security Prices (CRSP). We use the Bayesian approach developed by Sims and Zha (1998) to estimate the VAR model.[5] Because the sample starts from 1990:Q1, we consider a lag of 1 in the estimation.

[5]We have also used the ordinary least square (OLS) method to estimate the VAR model, for which investment, consumption, and hours worked are de-trended using the HP (Hodrick and Prescott (1997)) filter. The impulse response results are similar. Using the physical variance $\mathrm{Var}_t[\cdot]$ in the place of the risk-neutral variance generates similar impulse responses

Figure 1 presents the impulse responses of other variables to a positive one-standard-deviation shock to the conditional volatility of productivity growth. The results are obtained from the VAR estimation. The 68% error bands are also plotted in the figure. This figure shows that investment, consumption, and hours worked drop on impact, while the risk-neutral variance rises following the increase in the conditional volatility of productivity growth. These empirical results are consistent with Bloom (2009) and Gourio (2012) and suggest that, in times of high financial uncertainty, both aggregate consumption and output are low, whereas marginal utility is high from a representative agent's perspective. Because a high risk-neutral variance depresses investment, expected future consumption is low, leading to smaller future cash flows and lower equity valuation as a consequence. Further, Figure 1 indicates that the price-dividend ratio falls in response to a positive shock to the conditional volatility of productivity growth, and also that a high risk-neutral variance is associated with a low price-dividend ratio.

[Insert Figure 1 about here]

3 The Model

3.1 Preferences

We assume that the representative agent cannot observe state s_t in the Markov-switching model (1) but can learn about it through observing past realizations of productivity growth. The agent's posterior belief is given by the dynamic process decribed in (2). The non-observability of s_t captures the agent's ambiguity about the growth rate process. Following Ju and Miao (2012), we assume that the representative agent has generalized recursive smooth ambiguity preferences[6]

$$V_t = \left((1-\beta) U_t^{1-\frac{1}{\psi}} + \beta \left(\mathbb{E}_{\boldsymbol{\pi}_t} \left[\left(\mathbb{E}_{\{s_{t+1},t\}} \left[V_{t+1}^{1-\gamma} \right] \right)^{\frac{1-\eta}{1-\gamma}} \right] \right)^{\frac{1-\frac{1}{\psi}}{1-\eta}} \right)^{\frac{1}{1-\frac{1}{\psi}}} \tag{3}$$

[6] In the ambiguity literature, the smooth ambiguity approach differs from the multiple priors approach (for example, Gilboa and Schmeidler (1989) and Chen and Epstein (2002)) in that the multiple priors model features the max-min approach, which implies a tight link between ambiguity and ambiguity aversion. The smooth ambiguity model unravels this tight link, allowing for comparative statics analysis by holding the set of candidate models fixed, while varying the extent of ambiguity aversion. See Klibanoff et al. (2005, 2009) and Hayashi and Miao (2011) for more discussion.

for which the felicity function U_t depends on consumption (C) and labor hours (N) in the standard Cobb-Douglas form,

$$U_t = C_t \left(1 - N_t\right)^{\nu},$$

for which ν is the leisure preference.

With respect to preference parameters, $\beta \in (0, 1)$ is the subjective discount factor. Absent from ambiguity aversion, both parameters γ and ν control risk aversion with the labor margin (Swanson, 2012, 2018). More specifically, the degree of relative risk aversion is determined by $(\gamma - 1) + 1/(1 + \nu)$ *à la* Swanson (2012, 2018).[7] For this utility function, the elasticity of intertemporal substitution (EIS) is $\hat{\psi}$, $\hat{\psi} = (1 - (1 + \nu)(1 - 1/\psi))^{-1}$ (Gourio, 2012).

The degree of ambiguity aversion is governed by the parameter η. For the utility function (3), the agent is ambiguity averse if and only if $\eta > \gamma$. Expressed differently from recursive preferences with ambiguity neutrality, the certainty equivalent of smooth ambiguity utility is defined as,

$$\mathcal{R}_t \left(V_{t+1}\right) = \left(\mathbb{E}_{\boldsymbol{\pi}_t}\left[\left(\mathbb{E}_{\{s_{t+1},t\}}\left[V_{t+1}^{1-\gamma}\right]\right)^{\frac{1-\eta}{1-\gamma}}\right]\right)^{\frac{1}{1-\eta}} \tag{4}$$

for which $\mathbb{E}_{\{s_{t+1},t\}}[\cdot]$ denotes the expectation conditional on the history up to time t and a probability distribution of productivity growth given state s_{t+1}. In the certainty equivalent (4), the extra curvature in the preferences induced by the condition $\eta > \gamma$ precludes the compound reduction between the transition density and the conditional distribution of the growth rate.

For comparison, the certainty equivalent under ambiguity neutrality is based on the predictive distribution of Δa_{t+1} and expressed as,

$$\mathcal{R}_t \left(V_{t+1}\right) = \left(\mathbb{E}_t\left[V_{t+1}^{1-\gamma}\right]\right)^{\frac{1}{1-\gamma}} = \left(\int V_{t+1}^{1-\gamma} p\left(\Delta a_{t+1} | \boldsymbol{\pi}_t\right) d\left(\Delta a_{t+1}\right)\right)^{\frac{1}{1-\gamma}}$$

[7] Swanson (2012, 2018) rigorously examine the concept of "wealth-gamble risk aversion" in the presence of the labor margin. The agent with a flexible labor margin can absorb shocks to asset values along both the labor margin and the consumption margin, which can alter the agent's risk aversion. Swanson also notes that the coefficient of wealth-gamble risk aversion is related to the curvature of the agent's indirect utility function. As a result, the agent's wealth-gamble risk aversion naturally captures the additional curvature induced by ambiguity aversion. We demonstrate the influence of ambiguity aversion on the agent's wealth-gamble risk aversion in the Internet Appendix.

Meanwhile, the predictive density $p\left(\Delta a_{t+1}|z_t\right)$ is given by

$$p\left(\Delta a_{t+1}|\boldsymbol{\pi}_t\right) = \boldsymbol{\pi}_t \odot \boldsymbol{f}_{t+1}$$

The key property of the smooth ambiguity model is that it distinguishes ambiguity from ambiguity aversion (Klibanoff et al. (2005)). Ambiguity is drive by uncertainty in estimating the mean and volatility of productivity growth rate, both of which are not directly observable. Ambiguity aversion reflects the agent's attitudes toward such uncertainty. The more ambiguity averse the agent is, more weight is put on unfavorable states of productivity, which yield low continuation values.

3.2 Equilibrium characterization

Aggregate output (Y_t) is produced according to a standard constant-returns-to-scale, Cobb-Douglas production function:

$$Y_t = K_t^{\alpha}\left(A_t N_t\right)^{1-\alpha},\ \alpha \in (0,1),$$

for which α is the capital share, and K_t denotes the capital stock. Capital adjustment is costly. The law of motion for capital accumulation is,

$$K_{t+1} = (1-\delta)K_t + \phi\left(\frac{I_t}{K_t}\right)K_t, \tag{5}$$

and the adjustment cost function is given by (see Jermann (1998)):

$$\phi\left(\frac{I_t}{K_t}\right) = a_1 + \frac{a_2}{1-1/\xi}\left(\frac{I_t}{K_t}\right)^{1-1/\xi},\ a_2 > 0,\quad \xi > 0.$$

for which ξ is the elasticity of the investment rate to Tobin's Q, and the parameters a_1 and a_2 are chosen such that there is no adjustment cost in the steady state. The resource constraint is $Y_t = C_t + I_t$. The Internet Appendix provides a full characterization of the social planner's problem for this economy.

3.3 Asset Prices

Following Ju and Miao (2012) and Hayashi and Miao (2011), the stochastic discount factor (SDF) for the generalized recursive smooth ambiguity utility is:

$$M_{t,t+1} = \beta \left(\frac{C_{t+1}}{C_t}\right)^{-\frac{1}{\psi}} \left(\frac{1-N_{t+1}}{1-N_t}\right)^{\left(1-\frac{1}{\psi}\right)\nu} \left(\frac{V_{t+1}}{\mathcal{R}_t\left(V_{t+1}\right)}\right)^{\frac{1}{\psi}-\gamma} \left(\frac{\left(\mathbb{E}_{\{s_{t+1},t\}}\left[V_{t+1}^{1-\gamma}\right]\right)^{\frac{1}{1-\gamma}}}{\mathcal{R}_t\left(V_{t+1}\right)}\right)^{-(\eta-\gamma)}.$$

The last multiplicative term in the SDF reflects pessimism, due to ambiguity aversion. This pessimistic distortion to the SDF is endogenous and time-varying and makes the SDF more countercyclical. As a result, the model has potential to generate large equity premium and variance risk premium.

The risk-free rate, $R_{f,t}$, is the reciprocal of the expectation of the pricing kernel:

$$R_{f,t} = \frac{1}{\mathbb{E}_t\left[M_{t,t+1}\right]}$$

Following standard q-theory arguments, Tobin's q is expressed as,

$$q_t = \frac{1}{\phi'\left(\frac{I_t}{K_t}\right)}$$

for which ϕ' is the partial derivative of the adjustment cost function.

In RBC models, the firm's payout in period t is expressed as,

$$D_t^* = Y_t - w_t N_t - I_t = \alpha Y_t - I_t,$$

for which w_t is the equilibrium wage, and the second equality follows from the first order condition of labor: $w_t = \partial Y_t/\partial N_t = (1-\alpha)\, A_t^{1-\alpha} K_t^{\alpha} N_t^{-\alpha}$. The return on capital (investment), R_{t+1}^K, is:

$$R_{t+1}^K = \frac{1}{q_t}\left\{q_{t+1}\left[1-\delta_K+\phi\left(\frac{I_{t+1}}{K_{t+1}}\right)\right] + \frac{\alpha Y_{t+1} - I_{t+1}}{K_{t+1}}\right\}$$

In the absence of labor market frictions (e.g., search frictions or wage rigidity), the model implies

that the firm's payout is countercyclical: investment is high in good times and reduces the firm's payout, as the model is calibrated to reproduce high investment volatility. The counter-cyclicality of the payout greatly reduces the equity claim's riskiness and implies very low equity premium. In addition, the capital stock, as an important state variable, is slow-moving and thus does not imply high riskiness in the return on capital.

Because the stock market dividends only account for a small fraction of the payouts of production units (e.g., private equity, small businesses, real estate), we follow Bansal and Yaron (2004), Ju and Miao (2012), Kaltenbrunner and Lochstoer (2010), and Liu and Miao (2015), among others and assume that aggregate dividends are defined as a levered claim to aggregate consumption. In particular, we specify the dividend growth process as containing a component proportional to consumption growth and an independent component,

$$\Delta d_{t+1} \equiv \ln\left(\frac{D_{t+1}}{D_t}\right) = \lambda \Delta c_{t+1} + g_d + \sigma_d \varepsilon_{d,t+1} \tag{6}$$

for which $\varepsilon_{d,t+1}$ is an IID standard, normal random variable that is independent of all other shocks in the model. The parameter λ can be interpreted as the leverage ratio on expected consumption growth (see Abel (1999)). The parameters g_d and σ_d are calibrated to match the first and second moments of dividend growth in the data. This calibration implies that dividend growth is procyclical, in contrast to standard RBC models that depict such growth as countercyclical. This feature allows the model to better match equity premium and equity volatility in the data.

Stock returns, R_{t+1}, are defined as,

$$R_{t+1} \equiv \frac{P_{t+1} + D_{t+1}}{P_t} = \frac{1 + P_{t+1}/D_{t+1}}{P_t/D_t} \frac{D_{t+1}}{D_t}$$

and satisfy the Euler equation:

$$\mathbb{E}_t \left[M_{t,t+1} R_{t+1} \right] = 1$$

To solve for the price-dividend ratio, we rewrite the Euler equation as,

$$\frac{P_t}{D_t} = \mathbb{E}_t \left[M_{t,t+1} \left(1 + \frac{P_{t+1}}{D_{t+1}}\right) \frac{D_{t+1}}{D_t} \right]$$

Using the state variables to express the price-dividend ratio and setting $\frac{P_t}{D_t} = \xi\left(\tilde{K}_t, \boldsymbol{\pi}_t\right)$, the Euler equation becomes,

$$\xi\left(\tilde{K}_t, \boldsymbol{\pi}_t\right) = \mathbb{E}_t\left[M_{t,t+1}\left(1 + \xi\left(\tilde{K}_{t+1}, \boldsymbol{\pi}_t\right)\right)\exp\left(\Delta d_{t+1}\right)\right]$$

This functional equation can be solved by approximating the price-dividend ratio with Chebyshev polynomials in the state variables. The numerical method is explained in the Internet Appendix.

In the model, variance risk premium is defined as the difference between the risk-neutral and objective expectations of log stock return variance,

$$VRP_t = VIX_t^2 - VOL_t^2$$

where VIX_t^2 is the risk-neutral expectation of return variance, given by

$$VIX_t^2 = \frac{\mathbb{E}_t\left[M_{t,t+1}R_{t+1}^2\right]}{\mathbb{E}_t\left[M_{t,t+1}\right]} - \left(\frac{\mathbb{E}_t\left[M_{t,t+1}R_{t+1}\right]}{\mathbb{E}_t\left[M_{t,t+1}\right]}\right)^2$$

and VOL_t^2 is the objective expectation of return variance, given by

$$VOL_t^2 = \mathbb{E}_t\left[R_{t+1}^2\right] - \left(\mathbb{E}_t\left[R_{t+1}\right]\right)^2$$

4 Calibration

To calibrate the production economy to the historical data, we compute unconditional moments of quantities and asset returns for the period 1947:Q1—2016:Q1. The sample statistics include the standard deviations and correlations of investment, consumption, and output growth, as well as the first autocorrelation in consumption growth, the first and second moments of the risk-free rate and equity returns, and moments of VRP. Nominal returns are deflated by the CPI data from FRED at St.Louis. We then calibrate the model at a quarterly frequency. Because the model is nonlinear, no analytical solutions are available. We solve the model using numerical methods and then simulate the model. The quantitative results are based on 2,000 simulations. In solving and simulating the model, we consider pricing market dividends henceforth, unless otherwise stated.

4.1 Parameter choice

According to the RBC literature, we set the capital share at $\alpha = 0.36$ and the depreciation rate at $\delta = 0.02$. The leisure preference parameter ν in the felicity function is set at 2, such that the long-run mean proportion of labor hours is about 30%. We fix the parameter ψ at $\psi = 1.25$, which implies the EIS $\hat{\psi} = 2.5$, close to the values considered by Ai (2010), Gourio (2012) and Croce (2014) and the estimates reported by Schorfheide et al. (2018) and Gallant et al. (2019). In the benchmark calibration, the risk aversion parameter is set at $\gamma = 5$. The degree of risk aversion implied by this value is modest given the reasonable range of risk aversion advocated by Mehra and Prescott (1985). The capital adjustment costs parameter is set at $\xi = 6.5$ to deliver sufficiently high volatility of investment growth and low volatility of consumption growth. Finally, the subjective discount parameter β is chosen to imply a low mean, risk-free rate.

[Insert Table 2 about here]

The leverage parameter λ is set at 2.75, close to the values adopted by Abel (1999) and Bansal and Yaron (2004). The quarterly standard deviation of dividends growth is set at 5.5%, such that the calibrated models can match the equity volatility in the data. This value is close to those considered in other calibration studies (e.g., Bansal and Yaron (2004) and Ju and Miao (2012)). Further, the standard deviation of the independent shock in the dividend growth dynamics, σ_d, is set to match the volatility of dividend growth, which implies $\sigma_d = 0.053$, as the model implied volatility of consumption growth is about 0.45 percent per quarter. Following Bansal and Yaron (2004), g_d is chosen such that the average rate of dividends growth is equal to that of consumption growth, which delivers $g_d = -0.6\%$. The calibration implies that the contemporaneous correlation between consumption growth and dividends growth is about 0.2, close to the value that Kaltenbrunner and Lochstoer (2010) consider.

We choose the three-state Markov-switching model with ambiguity aversion and time-varying uncertainty as our benchmark model (AA3S) because this model can match well moments of quantities, asset returns and VRP simultaneously, compared to other calibrated models. For the purpose of model comparison, we also examine the following models: the three-state MS model with ambiguity aversion and constant volatility ($\overline{\text{AA3S}}$), the three-state MS model with Epstein-Zin's recursive

utility and time-varying uncertainty (EZ3S and $\widehat{\text{EZ3S}}$ for which $\widehat{\text{EZ3S}}$ features a high risk aversion).

For the benchmark model AA3S, we set the ambiguity aversion parameter at $\eta = 55$ to match the mean equity premium in the data. In the literature, there is no strict guidance on the choice of parameter values of η. The value of η commonly depends on specific contexts or applications. For example, Jahan-Parvar and Liu (2014) choose $\eta = 19$ for their model calibration at the annual frequency. Gallant et al. (2019) obtain various ranges of η estimates in consumption-based asset pricing models. Chen et al. (2014) assume $\eta = 60$ in analyzing dynamic portfolio choice under ambiguity.

Following Jahan-Parvar and Liu (2014), we use detection-error probabilities to calibrate the ambiguity aversion parameter η. Detection-error probabilities indicate the probability of making errors when distinguishing the reference model with the distorted model, by means of comparing likelihoods under the two models. To do so, we must simulate artificial data both from the reference model and the distorted model. The reference model is explicitly given by the regime-switching model (1) with empirically estimated parameters. To find the distorted model, we need to determine how ambiguity aversion distorts the "physical" transition probabilities. The Internet Appendix provides the characterization of distorted transition probabilities and details for computing detection-error probabilities. With a large value of η, the reference model (physical transition probabilities) looks very differently from the distorted model (distorted transition probabilities). Consequently, differentiating the two models proves easy, resulting in a small detection-error probability. Alternatively, we follow Ju and Miao (2012) and use thought experiments to calibrate ambiguity aversion.

The detection-error probability associated with $\eta = 55$ for the benchmark calibration is 5%.[8] The detection-error probability for model $\overline{\text{AA3S}}$ in which $\eta = 55$ is 26% and as such, higher than that for model AA3S. This result indicates that adding time-varying volatility in the three-state MS model makes the reference model more distinguishable from the distorted model and thus accommodates less scope of ambiguity. The main reason for the result is that with time-varying volatility conditional Gaussian likelihoods also differ in the second moment, which leads to easier detection of model distortion caused by ambiguity.

[8]Croce et al. (2012) also use a detection error probability of 5% in their benchmark calibration. Anderson et al. (2003) advocate a detection-error probability of 10% in models with robustness concerns.

4.2 Impulse responses

We perform impulse responses analysis to examine impacts of changes in productivity growth regimes for our benchmark three-state MS model. We assume that the economy remains in the second regime for a long time without the impact of innovation shocks. The capital stock and state belief vector stay at their steady-state levels accordingly. In the fifth period, productivity growth shifts from the second regime to the first regime, and following the regime shift, the productivity growth rate evolves according to the three-state MS model. We simulate productivity growth rates from the the three-state MS model after the regime shift, taking into account persistence of regimes characterized by the transition probabilities. We compute macroeconomic quantities and financial variables to investigate impulse responses to changes in state variables. Figures 2 and 3 plot mean responses of key variables across simulations.

Figure 2 shows that the regime shift causes the agent's belief to steer toward regime 1 that features low mean growth and high volatility while away from the other two regimes. Interestingly, upon impact of the shock in the fifth period, the conditional probability of regime 2 rises slightly for that period, and that of regime 1 rises moderately, whereas the agent believes that regime 3 becomes significantly less likely to occur. This is due to the fact that both regime 1 and regime 2 are "worse" regimes compared to regime 3. After the regime switching has occurred, persistence of regimes drives down the conditional probability of regime 2 sharply. Meanwhile, the agent's belief that regime 1 persists is further strengthened. The conditional probability of regime 3 reverts toward the stationary level. It is worth mentioning that these results are absent in the two-state MS model that is commonly used in asset pricing studies. The responses of the agent's belief deliver the dynamics of conditional mean and volatility of productivity growth observed in Figure 2, i.e., conditional mean drops whereas conditional volatility increases. In addition to the Bayesian belief, we also plot the ambiguity-distorted belief in Figure 2. We observe that in this case ambiguity aversion raises the conditional probability of regime 1 but decreases that of regime 3, and thus the endogenous pessimism leads to lower conditional mean growth rates and higher conditional volatilities.

[Insert Figure 2 about here]

Figure 3 plots responses of macroeconomic quantities and financial variables. The consumption and investment series are de-trended in the plots. Due to the permanent impact of the regime shift on the productivity level, both investment and consumption decrease significantly and move toward the new but lower steady-state levels respectively. Hours worked also decrease as a result. Because of the regime shift, the marginal product of capital drops, leading to the observed decline in Tobin's q. Additionally, expected future consumption growth must decline as a consequence of lower levels of investment and the deteriorated belief about economic regimes. According to Kaltenbrunner and Lochstoer (2010) and Croce (2014), the persistent movement in expected consumption growth generates the long-run risk effect on asset prices in production economies.

[Insert Figure 3 about here]

The regime shift in productivity growth raises marginal utility of the agent through the short-run and long-run channels and, in turn, leads to an increase in the SDF. More important, ambiguity aversion greatly magnifies the response of the SDF because of the endogenous pessimism. The sharp rise in the SDF and the negative impact on expected future dividends together lead to a large decline in the price-dividend ratio and therefore in the realized equity return. The negative correlation between the SDF and the realized return implies a large and positive equity risk premium associated with the regime switching. Both the conditional equity premium and the equity volatility rise significantly because the impact of a pessimistic change in the state belief is reinforced under ambiguity aversion. Moreover, because both the SDF and conditional equity volatility increase under the regime shift, the multiplier effect raises the risk-neutral variance (VIX^2) by a larger amount, resulting in a substantial volatility risk premium, as shown in the last plot in Figure 3. Without time-varying volatility of productivity growth, VIX^2 rises moderately in response to the regime shift, and thus, the resulting variance risk premium is close to zero.

The impulse responses analysis suggests that regime switching in productivity growth and learning together drive countercyclical variation in the risk-neutral variance. The analysis also suggests that the time-varying productivity volatility is important for generating significant movement in the risk-neutral variance and rationalizing the large variance risk premium observed in the data. These results directly support our findings in Section 2: 1) the empirically observed negative impacts of the risk-neutral variance on quantities are driven by the time-varying volatility of productivity

growth; 2) financial uncertainty proxied by the risk-neutral variance is negatively priced and carries a positive risk premium.

To better understand our findings, we apply the empirical method in Section 2 to estimate the VAR model using data simulated from the benchmark model AA3S. We simulate 2,000 samples and estimate the VAR model on simulated conditional volatility of productivity growth, risk-neutral variance, consumption, investment, hours worked, and the price-dividend ratio. For each estimation of the VAR model, we perform the impulse responses analysis to examine the impact of an increase in conditional volatility of productivity growth. Results are presented in Figure 4. The figure provides a comparison between model-generated results and empirical results reproduced from Figure 1. We find that our benchmark model can closely replicate empirical facts observed in the actual data. That is, an increase in conditional volatility of productivity growth leads to lower levels of quantities (consumption, investment and hours worked) and the price-dividend ratio, while results in a rise in uncertainty proxied by the risk-neutral variance. In Figure 4, the mean level of the VAR impulse responses generated from model simulations is close to results for the empirical data, and moreover, the plots for the empirical data are bounded within the 2.5% and 97.5% of the simulated impulse responses for the benchmark model. These results suggest that our model can explain findings documented in previous literature (e.g., Bloom (2009) and Bloom et al. (2018)) that uncertainty measured by the risk-neutral variance dampens real economic activity.

[Insert Figure 4 about here]

4.3 Quantitative results

4.3.1 Unconditional moments

Table 3 summarizes the annualized moments for macroeconomic quantities and asset returns. With respect to Table 3, we observe the following: (1) the volatility of consumption growth is low ($\sigma_{\Delta c} = 1.06\%$), (2) the volatility of investment growth is much higher ($\sigma_{\Delta i} = 4.87\%$), (3) comovements among aggregate quantities exist, (4) the risk-free rate is low and smooth, and (5) the equity premium and volatility are high ($\mathbb{E}(R - R_f) = 6.23\%$ and $\sigma(R - R_f) = 15.26\%$). Regarding the variance risk premium (in monthly squared percentage), we observe that (1) the VRP has high mean

($\mathbb{E}(VRP) = 11.08$ in the full sample period (1990—2016)) and high volatility ($\sigma(VRP) = 23.62$), and (2) the skewness is positive and the excess kurtosis is high, suggesting that the VRP has fat tails.[9]

[Insert Table 3 about here]

We first present macroeconomic and financial moments for the benchmark model AA3S that features time-varying volatility and ambiguity aversion and then proceed to compare these results with models under alternative assumptions. Table 3 shows that model AA3S can match moments of quantities well. The volatility of consumption growth in the model is close to the post-war data and is about 1%. Matching consumption volatility in the data is important in the first place because production-based models aim to reconcile high equity premium with low consumption risk. The post-war consumption data exhibits moderate persistence with autocorrelation $\rho(\Delta c_t, \Delta c_{t+1}) = 0.29$. Due to that productivity growth regimes are persistent and that the agent's learning produces persistent beliefs, the model also generates autocorrelation in consumption growth.

Because adjustment costs are assumed to be low ($\xi = 6.5$) and the EIS is high ($\psi = 2.5$), investment growth is volatile, about four times the volatility of consumption growth. A high EIS increases the intertemporal substitution effect and makes savings more appealing in high productivity states. With endogenous labor hours, the correlation between consumption growth and investment growth ($\rho(\Delta c, \Delta i) = 0.45$) closely matches the data, a result not present in models with exogenous labor choice (for example, see Kaltenbrunner and Lochstoer (2010) and Liu and Miao (2015)). The correlations of output growth with consumption growth and investment growth ($\rho(\Delta c, \Delta y) = 0.69$ and $\rho(\Delta i, \Delta y) = 0.95$) are also close to the corresponding moments in the data.

With respect to financial moments, the model produces low mean and volatility of the risk-free rate due to the high EIS value imposed in the calibration.[10] The ability of the model in matching moments of the risk-free rate suggests that the model delivers reasonable dynamics of the SDF. With a modest degree of risk aversion, model AA3S generates a high mean equity premium of 5.67 percent per year that is close to the data moment. The volatility of excess returns in the model is

[9]The moments of VRP for the pre-crisis period 1990–2007 are similar.

[10]In production-based models with long run risks, the impacts of the EIS parameter on both quantities and asset prices are noteworthy, see Croce (2014). With lower values of ψ, the volatility of consumption growth rises and the volatility of investment growth falls significantly. Furthermore, the comovement between conditional variance of returns and the SDF is not strong enough, leading to a low and smooth VRP.

also high at about 17 percent because financial moments are computed based on the specification of exogenous market dividends (Equation (6)). For model AA3S, ambiguity aversion greatly increases variation in the SDF and implies a high market price of risk. The unconditional market price of risk $\sigma(M)/\mathbb{E}(M)$ is high at 0.54. The model implied mean equity premium is therefore positive and high given that the conditional correlation between the SDF and realized return is negative.

Remarkably, the benchmark model AA3S produces a high unconditional mean of the VRP ($\mathbb{E}(VRP) = 14.56$) that closely matches the data. The standard deviation of the VRP implied by the model is 13.34, which is below that reflected in the data (i.e., 23.62 for the full sample period) but indicates that the model-generated VRP is volatile. Consistent with the data, the model generates a non-Gaussian distribution of VRP, with a skewness measure of 3.36 and an excess kurtosis of 15.23, both of which are close to the corresponding moments in the data. These results suggest that variance risk is correctly priced in the benchmark model with time-varying volatility and ambiguity aversion. Time-varying productivity volatility accounts for a substantial amount of variance risk in equity returns. Moreover, ambiguity aversion distorts the risk-neutral measure and makes the agent be more concerned with variance risk. Thus, the risk-neutral variance is greatly magnified in the model.

To examine the role of key assumptions of the model, we investigate three alternative models, $\overline{\text{AA3S}}$, EZ3S and $\widehat{\text{EZ3S}}$.[11] In comparison with the benchmark model, model $\overline{\text{AA3S}}$ assumes constant volatility of productivity growth and model EZ3S assumes Epstein-Zin's recursive utility without ambiguity aversion. Table 3 shows that volatilities of quantities are smaller in model $\overline{\text{AA3S}}$ than in model AA3S. Investment volatility is greatly downplayed when time-varying productivity volatility is shut down.

We find that suppressing time-varying productivity volatility has substantial impacts on the equity premium and the variance risk premium. Model $\overline{\text{AA3S}}$ generates a mean equity premium that is only about half of that in model AA3S. This result is consistent with the finding in previous literature that volatility risk carries a significant amount of risk premium, for example see Bansal and Yaron (2004), Drechsler and Yaron (2011), and Drechsler (2013). On the other hand,

[11] For comparison, we have also solved models with and without ambiguity aversion, assuming that productivity growth follows the two-state MS process specified in Section 2.2. However, when these models are calibrated to match the historical equity premium, the implied mean and volatility of VRP are too low. See the Internet Appendix for related results.

studies such as Veronesi (1999), Cogley and Sargent (2008) and Ju and Miao (2012) suggest that in consumption-based models with regime switching growth rates, learning about the mean growth state can lead to large uncertainty about the state of the economy and therefore high market price of risk, even in the absence of time-varying volatility. Our analysis contributes to the existing literature by showing that time-varying volatility still accounts for a significant magnitude of risk premium in the framework of regime switching productivity growth and learning. Results in Table 3 further indicate that the market price of risk implied by model $\overline{\text{AA3S}}$ is about half of that in the benchmark model.

More importantly, the impact of time-varying volatility on variance risk premium is pronounced. In contrast to model AA3S, the unconditional mean of VRP implied by model $\overline{\text{AA3S}}$ is close to zero ($\mathbb{E}(VRP) = 0.26$), and the volatility of VRP is also very low ($\sigma(VRP) = 0.39$). In addition, the model implies a much lower skewness, contrary to the data. Although the unconditional volatility of returns is roughly the same in both models (AA3S and $\overline{\text{AA3S}}$), volatility risk is priced significantly different in these two models. Because model $\overline{\text{AA3S}}$ lacks time-varying productivity volatility, there is inadequate comovement of the SDF and volatility of returns. As a result, volatility risk in returns is not sufficiently priced in this model.

We suppress ambiguity aversion by assuming $\eta = \gamma = 5$ and obtain model EZ3S. This model generates similar dynamics of quantities compared to the benchmark model AA3S. However, both the equity premium and the variance risk premium implied by the model are small due to that the lack of endogenous pessimism results in a low market price of risk. These results confirm a key aspect of model EZ3S: business cycle fluctuations are unable to create large variations in the SDF and strong comovement of the SDF and conditional volatility of returns. An interesting question here is: can Epstein-Zin's recursive utility model with a high degree of risk aversion generate empirically reasonable asset pricing implications? In model $\widehat{\text{EZ3S}}$, the ambiguity-neutral agent has recursive utility with a high aversion ($\gamma = 10$). We find that both the equity premium and the VRP implied by this model are still lower than those in the benchmark model. More importantly, as shown by Gallant et al. (2019), estimates of risk aversion are more reasonable once ambiguity aversion is taken into account in estimating asset pricing models.

4.3.2 Conditional VIX^2

In our benchmark model, changes in the agent's belief under time-varying volatility and ambiguity aversion are important for generating the volatility dynamics of returns and pricing the variance risk. As such, we investigate conditional VIX^2 and VRP for different values of the belief vector $\boldsymbol{\pi}$. We compare the benchmark model AA3S with alternative models to understand the impacts of time-varying volatility and ambiguity aversion separately. In the analysis, we assume that capital is at its long run mean in the simulation and that the filtered probability of state 3 (the good state) remains at its steady-state level. As the agent's belief about state 1 (the bad state) changes, uncertainty about the state of the economy varies and we compute conditional market price of risk, VOL^2, VIX^2 and VRP in different scenarios. Figure 5 plots these conditional moments as functions of the filtered probability of state 1 for the three models mentioned above.

[Insert Figure 5 about here]

Figure 5 shows that the benchmark model produces the highest conditional moments among all the four models, indicating its success in reproducing high market price of risk and VRP present in the data. For models with time-varying volatility (AA3S, EZ3S and $\widehat{\text{EZ3S}}$), the conditional volatility of returns is increasing in π_1, whereas the relation is almost flat for model $\overline{\text{AA3S}}$ (see Panel B). The result implies that without time-varying volatility of productivity growth, conditional volatility of returns is small and smooth, which leads to little variance risk being priced. This scenario is alleviated to some extent in models EZ3S and $\widehat{\text{EZ3S}}$ but is still not as significant as in model AA3S. Drechsler (2013) provides related results in an endowment setting and shows that time-varying consumption volatility is important for generating large volatility risk in returns.

When we plot the conditional market price of risk, $\sigma_t(M)/\mathbb{E}_t(M)$, against π_1, the plot displays a humped shape for models AA3S and $\overline{\text{AA3S}}$ but not for EZ3S or $\widehat{\text{EZ3S}}$. Previous studies such as Veronesi (1999) and Ju and Miao (2012) also obtain hump-shaped market prices of risk plotted against state probabilities in two-state MS models. The feature that we observe in Figure 5 Panel A suggests that the agent's concern about state uncertainty first rises and then falls when he is ambiguity averse. In the simulation, the value of π_1 is usually small at around 0.03 if the growth rate of productivity is more likely to be drawn from normal states. When a severe shock to productivity

growth occurs, the agent updates his belief about the three regimes accordingly and thus π_1 rises. If the agent's preferences are represented by Epstein-Zin's recursive utility, the market price of risk rises only modestly. However, ambiguity aversion can greatly magnify concern about state uncertainty and result in a sharp increase in the market price of risk.

Either without time-varying volatility or ambiguity attitudes, a negative shock to productivity growth cannot raise the risk-neutral variance (VIX^2) substantially higher than the conditional variance of returns (VOL^2) because the variance risk is not significantly priced. Thus, in both models $\overline{\text{AA3S}}$ and EZ3S, VIX^2 and VOL^2 are not responsive to variations of productivity growth, and the variance risk premium is small. Model $\overline{\text{AA3S}}$ performs better in this respect but is still not as good as model AA3S. By contrast, in model AA3S the endogenous pessimism and large variation in conditional variance of returns together imply high and volatile VIX^2, as is evident in Panel C and D in Figure 5. Thus, the model is able to generate empirically plausible dynamics of the variance risk premium.

4.3.3 The term structure of implied volatilities

The risk-neutral variance (VIX^2), in practice, is computed as the weighted sum of out-of-the-money (OTM) index option prices[12]. In fact, large variance risk premium arises because OTM put options are, measured by implied volatility (IV), much more expensive than at-the-money options. This pattern is the well known implied volatility skew (smirk) in index options. To the extent that our benchmark model is able to generate a sizable VRP, it is interesting to examine whether our model is also able to generate the implied volatility skew. Moreover, we also compare our model's IV skew with that in the data across different maturities to study the term structure effect, because Dew-Becker et al. (2017) shows that the variance risk behaves differently across maturities.

In our model, the value of a call option expiring in n periods, $Call_t^{(n)}$, is given by the expectation of the option's future cash flow multiplied by the multi-period SDF:

$$Call_t^{(n)} = E_t \left[M_{t,t+n} \max \left(0, P_{t+n} - K \right) \right], \tag{7}$$

where P_{t+n} is the price of the underlying asset at time $t+n$, K is the option's strike price, and $M_{t,t+n}$

[12]Please see https://www.cboe.com/micro/vix/vixwhite.pdf.

is the multi-period SDF, $M_{t,t+n} = M_{t,t+1}M_{t+1,t+2}\cdots M_{t+n-1,t+n}$ in which $M_{t,t+1}$ is the one-period SDF. The value of a put option, $Put_t^{(n)}$, can be calculated in a similar way but for the put option's future cash flow. We calculate prices of call and put options that are 1–4 quarters till maturity at the steady state for different moneyness. We compute option prices numerically by Monte Carlo simulations with 20,000 sample paths. Along each simulated path, we obtain realized $M_{t,t+n}$ and $\max(0, P_{t+n} - K)$. We then use the steady-state belief vector $\boldsymbol{\pi}_{ss}$ and transition probabilities to compute the expectation.

For each maturity, we price options with a wide range of moneyness and compute the implied volatility for each option. Figure 6 plots the option implied volatilities generated by our benchmark AA3S model against moneyness. For comparison, we also plot the implied volatilities generated under alternative models ($\overline{\text{AA3S}}$, EZ3S, and $\widehat{\text{EZ3S}}$) and compare all models with the average implied volatilities in the data. The 4 panels graph the implied volatility skew of options with time to maturity ranging from 1 to 4 quarters. To study the term structure of the IV skew, we measure moneyness by Black-Scholes call delta instead of the ratio of stock price over strike price because a given stock over strike ratio is not directly comparable across maturities. For example, options with call delta equals 10 percent are OTM calls with high strike prices and options with 90 percent call delta are in-the-money (ITM) calls with low strike prices. Because of put-call parity, the implied volatility of the 90 percent delta call option is the same as that of an OTM put option with the same strike price[13]. Therefore, plotting the IV against call delta (from high to low) is equivalent with plotting the IV against strike price (from low to high).

In the historical data, we find the familiar pattern of high delta (low strike) OTM put options having higher IVs than ATM options. For example, for 1-quarter options, the average historical IV for 80 delta option (OTM put) is 0.232 and that for 50 delta option is 0.184. The IVs of the same maturity and moneyness generated by our benchmark model are 0.232 and 0.165, respectively. The benchmark model generates an implied volatility skew, with the implied volatility monotonically decreasing from high to low deltas (or from low to high strike prices) and the skew is as steep as that in the data. On the other hand, the 80 delta IVs generated by the $\overline{\text{AA3S}}$, EZ3S, and $\widehat{\text{EZ3S}}$ models are all much lower at 0.147, 0.139, and 0.171, respectively. Under these alternative models, the IV

[13]To be precise, the Black-Scholes delta of a put option is negative. As a result, we always use the delta of the call option which has the same strike price as the put.

skews are much flatter than the skew in our benchmark model and that in the data, highlighting the importance of the time-varying macroeconomic uncertainty and role of ambiguity aversion. For options with 2 to 4 quarters to maturity, the IV skews in the data look similar with that of 1-quarter options. The similarity across maturities is because we plot the skew against delta instead of the ratio of stock price over strike. The IV term structure in the data is on average upward sloping, also consistent with the finding in Dew-Becker et al. (2017). Across the entire term structure, our benchmark model continues to generate the best fit of the IV skew.

[Insert Figure 6 about here]

To be more precise, we compare the model generated implied volatilities with those in the data with a regression approach. For each maturity, we regress the historical average implied volatility at each moneyness (delta) level on the model generated implied volatility of the same moneyness and the results are presented in Table 4. Ideally, the intercept should be 0 and the coefficient for the model implied volatility should be equal or close to 1. For our benchmark model shown in Panel A, the coefficients for the model IV are 0.735, 0.994, 0.993, and 1.056 for the 4 maturities, respectively. Only the coefficient on the 1-quarter option is significantly different from 1. The intercepts are 0.059, 0.021, 0.012, and -0.003 across all 4 maturities. The intercepts are insignificantly different from 0 for maturities longer than 2 quarters. As we compare the fit across maturities, the intercepts are getting closer to 0, the coefficients are getting closer to 1, and the R^2s are increasing from short to long maturities. These results suggest that our benchmark model explains the implied volatilities even better at longer maturities. Panels B, C, and D present the regressions using the $\overline{\text{AA3S}}$, EZ3S, and $\widehat{\text{EZ3S}}$ models, respectively. For all 3 alternative models across all 4 maturities, all coefficients are very large and significantly different from 1 and all intercepts are negative and significantly different from 0. For the 2 models without ambiguity aversion (EZ3S and $\widehat{\text{EZ3S}}$), the R^2s decline and the coefficients (intercepts) move further away from 1 (0) as maturities increase. Overall, the term structure analysis shows that our benchmark model explains the IV skew across all maturities and highlights the important role of ambiguity aversion.

[Insert Table 4 about here]

4.3.4 Cross correlations

We follow Gourio (2012) and plot cross-correlations to study the relations between the risk-neutral variance and macroeconomic and financial variables. Figure 7 (the dashed line) plots the correlations between the risk-neutral variance and consumption growth, investment growth, hours growth, and the equity return, respectively at different leads and lags (i.e., $Corr\left(\text{Var}_t^Q\left[R_{t+1}\right], x_{t+k}\right)$ for $k = -6$ to 6). Unlike the levels in these macroeconomic quantities, the growth rates in these variables are not persistent at quarterly frequency. The solid line plots the counterparts implied by our benchmark model. For the model implied correlations, we simulate 2,000 sample paths under the benchmark model and compute the distributions of the correlations. The solid line denotes the average correlations and we also plot the 2.5 and 97.5 percentiles of the cross correlations in the simulations. In general, all the cross correlations are v-shaped. For aggregate consumption growth, investment growth, and hours growth, these correlations are negative for small negative k, suggesting that consumption and investment negatively impact risk-neutral variance. In other words, good times with fast consumption and investment growth tend to lower financial uncertainty in the future. More interestingly, the correlations between the risk-neutral variance and growth rate in quantities (e.g. consumption, investment, and hours) are all negative for $k > 0$, suggesting that high financial uncertainty tends to dampen future real economic activity, consistent with the findings in Bloom (2009). The lead-lag relations between the risk-neutral variance and the equity return suggest that the stock market performance negatively contributes to the level of financial uncertainty (i.e., high past returns lead to low, current risk-neutral variance). The model implied cross correlations closely fit those observed in the data. The negative correlations in the data are particularly strong for investment growth and equity returns. These results are consistent with the mechanism in which a bad shock to expected productivity growth or an increase in conditional productivity volatility simultaneously raises risk-neutral variance and lowers the price-dividend ratio; in turn, this low current price-dividend ratio implies a high expected return. Thus, this result and mechanism help explain the finding in Bali and Zhou (2016) that the uncertainty proxied by VIX is negatively related to equity valuation and carries a positive premium.

[Insert Figure 7 about here]

Since the model features time-varying volatility of productivity growth, we next examine the link between financial uncertainty and macroeconomic uncertainty. We estimate the conditional volatilities of consumption growth, investment growth, hours growth, and equity returns using a 40-quarter moving window. The conditional volatilities proxy for macroeconomic uncertainty. For comparison, we simulate 2,000 sample paths under the benchmark model and compute the macroeconomic uncertainty the same way as in the data. Hence, we can compute the cross correlations of financial uncertainty and macroeconomic uncertainty in each simulated path and obtain a distribution of the cross correlations under our benchmark model. Figure 8 (the dashed line) plots the correlation between the risk-neutral variance and volatilities of consumption growth, investment growth, and hours growth at different leads and lags (i.e., $Corr\left(\mathrm{Var}_t^Q\left[R_{t+1}\right], \sigma_{x,t+k}\right)$ for $k = -6$ to 6). We note that for small $k > 0$, this correlation is significantly positive, suggesting that the risk-neutral variance positively forecasts future volatility of quantities. The correlations are also positive for $k \leq 0$, indicating that high macroeconomic uncertainty also raises high financial uncertainty. Moreover, the correlation between the risk-neutral variance and stock market return volatility shows a pronounced tent-shaped pattern, in Panel D of Figure 8. Our empirical results suggest that the relation between the two types of uncertainty is very strong. Overall, the cross correlations in our benchmark model closely resemble those observed in the data, suggesting that our production-based general equilibrium model successfully explain these important stylized facts. However, alternative models lacking time-varying volatility are unable to rationalize these empirical phenomena due to insignificant time variations in macroeconomic volatilities and the risk-neutral variance.

[Insert Figure 8 about here]

4.4 Limitations and future research

Our model is successful in matching the risk-neutral variance, the VRP, the term structure of variance risk, and other empirical regularities. At the same time, we are mindful of the model's limitations. Our calibration results hinge on an exogenous dividend process that features a levered claim on aggregate consumption. Not surprisingly, asset pricing results become much weaker when dividends are endogenously determined as in a RBC model. Even after introducing financial lever-

age in the analysis, equity premium is only about 1.7% in the AA3S model, with equity volatility about 3.8% and VRP about 1. Alternative calibrations have both equity premium and VRP close to 0. The related results are presented in the Internet Appendix.

In addition, we use the historical TFP growth rate to estimate the conditional probabilities of the 3 regimes and then further compute the time series of the model implied VIX^2 and VRP. The contemporaneous correlation between the model implied VIX^2 and the historical VIX^2 is about 0.37 ($p = 0.00$). In the contemporaneous regression of the historical VIX^2 on the model implied VIX^2, the R^2 is 13%. The correlation between our model implied VRP and historical VRP is 0.18 ($p = 0.06$) and the contemporaneous regression R^2 is 1%. Overall, these results suggest that the time variation in conditional mean or volatility of productivity growth can only partially explain the variation in the historical VIX^2 and VRP. More details are presented in the Internet Appendix. In light of these limitations, future research could explore the variance risk premium in production economies along potentially fruitful avenues such as labor market frictions (Favilukis and Lin, 2015), irreversible investment (Bloom et al., 2018), parameter learning (Collin-Dufresne et al., 2016), or macroeconomic announcements (Ai and Bansal, 2018).

5 Conclusion

We have studied a production-based asset pricing model with regime-switching productivity growth, learning and ambiguity. Both mean and volatility of the growth rate of productivity are assumed to follow a Markov chain with an unobservable state. The representative agent learns about the state through observing realizations of the growth rate. The agent's utility preferences are characterized by the generalized recursive smooth ambiguity preferences. Ambiguity arises due to uncertainty faced by the agent in the estimation of the unobservable state, and the agent is averse to this uncertainty. Ambiguity aversion implies pessimistic distortion to the subjective belief and has important asset pricing implications. We consider the model with a three-regime Markov-switching process as our benchmark model and compare it to alternative models with constant volatility, Epstein-Zin's recursive utility and a two-regime Markov-switching process respectively.

Our benchmark model with modest risk aversion can match both macroeconomic and financial

moments well. Importantly, the model generates moments of the variance risk premium close to the data. Moreover, the model can reconcile empirical regularities about the relations between the risk-neutral variance and levels and volatilities of quantities respectively. The interplay between productivity volatility risk and ambiguity aversion is important in explaining these stylized facts and pricing variance risk in returns. This modeling feature is not present in previous studies on smooth ambiguity and asset pricing such as Ju and Miao (2012), Miao et al. (2018), Collard et al. (2018) and Jahan-Parvar and Liu (2014).

Table 1: **Parameter Estimates of the Markov-switching Model**

Panel A: two-regime Markov-switching model

μ_1	μ_2	σ_1	σ_2	p_{11}	p_{22}
-0.989	1.026	3.726	1.007	0.753	0.977
(0.100)	(0.112)	(1.320)	(0.140)	(0.003)	(0.037)

Panel B: three-regime Markov-switching model

μ_1	μ_2	μ_3	σ_1	σ_2	σ_3
-0.610	0.821	1.967	3.674	1.021	0.597
(0.004)	(0.035)	(0.001)	(0.006)	(0.001)	(0.030)

p_{11}	p_{13}	p_{21}	p_{22}	p_{31}	p_{33}
0.670	0.324	0.018	0.952	0.085	0.645
(0.004)	(0.004)	(0.037)	(0.037)	(0.007)	(0.007)

Panel C: Model selection

	LL	BIC
two-regime MS	1040.242	-2046.632
three-regime MS	1047.968	-2028.233

This table reports the maximum likelihood estimates of parameters in the Markov-switching model (1). Data for estimation are quarterly total factor productivity growth rates from 1947:Q1 to 2016:Q1. Panel A presents the estimated parameters of a two-regime Markov-switching model and Panel B presents those of a three-regime model. Panel C presents the log-likelihood (LL) and Bayesian information criterion (BIC) of the two-regime and three-regime models. The estimates are obtained using the expectation maximization algorithm developed by Hamilton (1990). Standard errors are reported in parentheses.

Table 2: **Benchmark Parameter Choices**

Parameter	Description	Value
β	Subjective discount factor	0.9975
γ	Risk aversion	5
$\hat{\psi}$	EIS	2.5
η	Ambiguity aversion	55
ν	Leisure preference	2
α	Capital share	0.36
δ	Depreciation rate	0.02
ξ	Adjustment cost parameter	6.5
λ	Leverage	2.75

Table 3: **Calibration Results: Models with the Three-regime MS Process**

	Data	AA3S	$\overline{\text{AA3S}}$	EZ3S	$\widehat{\text{EZ3S}}$
Panel A: Macroeconomic moments					
$\sigma_{\Delta c}$ (%)	1.06	0.96	0.93	0.92	0.96
$\sigma_{\Delta i}$ (%)	4.87	4.20	3.09	4.13	4.28
$\sigma_{\Delta y}$ (%)	2.56	1.85	1.51	1.84	1.86
$\rho(\Delta i, \Delta y)$	0.71	0.95	0.94	0.96	0.95
$\rho(\Delta c, \Delta y)$	0.46	0.69	0.73	0.74	0.67
$\rho(\Delta c, \Delta i)$	0.42	0.45	0.46	0.53	0.42
$\rho(\Delta c_t, \Delta c_{t+1})$	0.29	0.19	0.13	0.20	0.19
Panel B: Financial moments					
$\mathbb{E}[R_f] - 1$ (%)	1.04	1.74	1.93	1.96	1.80
$\sigma(R_f)$ (%)	0.78	0.22	0.19	0.20	0.23
$\mathbb{E}(R - R_f)$ (%)	6.23	5.67	2.68	1.38	3.29
$\sigma(R - R_f)$ (%)	15.26	17.39	16.11	14.15	15.95
$\mathbb{E}(VRP)$	11.08	14.56	0.26	1.06	5.19
$\sigma(VRP)$	23.62	13.34	0.39	2.35	8.17
Skewness (VRP)	2.33	3.36	0.62	5.89	4.62
Kurtosis (VRP)	10.23	15.23	11.22	44.55	26.88
$\sigma(M)/\mathbb{E}(M)$	n.a.	0.54	0.27	0.10	0.23

This table reports unconditional moments for the benchmark model AA3S and alternative models. The growth rate of productivity follows a three-regime Markov-switching model, and the parameter estimates are shown in Table 1. Parameter choices for model AA3S are shown in Table 2. Model $\overline{\text{AA3S}}$ differs from AA3S in that the innovation shock to productivity growth has constant volatility ($\sigma(s_t) = \sigma$). Model EZ3S features ambiguity neutrality ($\gamma = \eta$). Model $\widehat{\text{EZ3S}}$ differs from EZ3S by assuming $\gamma = 10$. The results are based on 2,000 simulations, and each simulation contains 400 quarters of data.

Table 4: **The Term Structure of Implied Volatility**

	1Q	2Q	3Q	4Q
Panel A: Model AA3S				
Const	0.0588	0.0212	0.0123	-0.0028
t-stat	(8.4232)	(2.6178)	(1.7177)	(-0.3960)
β	0.7348	0.9944	0.9925	1.0560
t-stat	(19.7565)	(22.0294)	(26.3220)	(29.4880)
t-stat (β=1)	(-7.1314)	(-0.1247)	(-0.1977)	(1.5632)
R^2	0.9605	0.9680	0.9774	0.9819
Panel B: Model $\overline{\text{AA3S}}$				
Const	-2.7353	-1.6405	-1.4029	-1.2749
t-stat	(-16.8194)	(-21.9056)	(-47.0844)	(-51.6707)
β	20.2405	12.8948	11.0568	10.0689
t-stat	(18.0060)	(24.5334)	(53.7508)	(59.7674)
t-stat (β=1)	(17.1164)	(22.6308)	(48.8894)	(53.8315)
R^2	0.9528	0.9741	0.9945	0.9955
Panel C: Model EZ3S				
Const	-0.3545	-0.5530	-0.5855	-0.6549
t-stat	(-11.7199)	(-14.1903)	(-13.0367)	(-11.3762)
β	4.1682	5.8270	5.9904	6.4843
t-stat	(18.1259)	(19.2514)	(17.4674)	(14.8510)
t-stat (β=1)	(13.7773)	(15.9476)	(14.5515)	(12.5606)
R^2	0.9534	0.9585	0.9500	0.9321
Panel D: Model $\widehat{\text{EZ3S}}$				
Const	-0.0389	-0.1148	-0.1228	-0.1351
t-stat	(-2.6843)	(-5.8794)	(-5.9739)	(-6.0245)
β	1.5497	2.1593	2.1703	2.2362
t-stat	(16.1418)	(16.0340)	(15.7078)	(14.9879)
t-stat (β=1)	(5.7255)	(8.6085)	(8.4701)	(8.2854)
R^2	0.9419	0.9412	0.9389	0.9332

This table examines whether our model or other benchmark models can explains the observed SPX option implied volatility across moneyness at different maturities using the regression approach. We regress SPX option implied volatilities across moneyness on the model generated option implied volatilities of the same moneyness. We repeat this for each maturity and each column shows the results using options of a given maturity. Panel A shows the regression using the IV from the AA3S model. Panel B shows the regression using IV from the $\overline{\text{AA3S}}$ model. Panel C shows the regression using the IV from the EZ3S model. Panel D shows the regression using the IV from the $\widehat{\text{EZ3S}}$ model.

Figure 1: **VAR impulse responses**

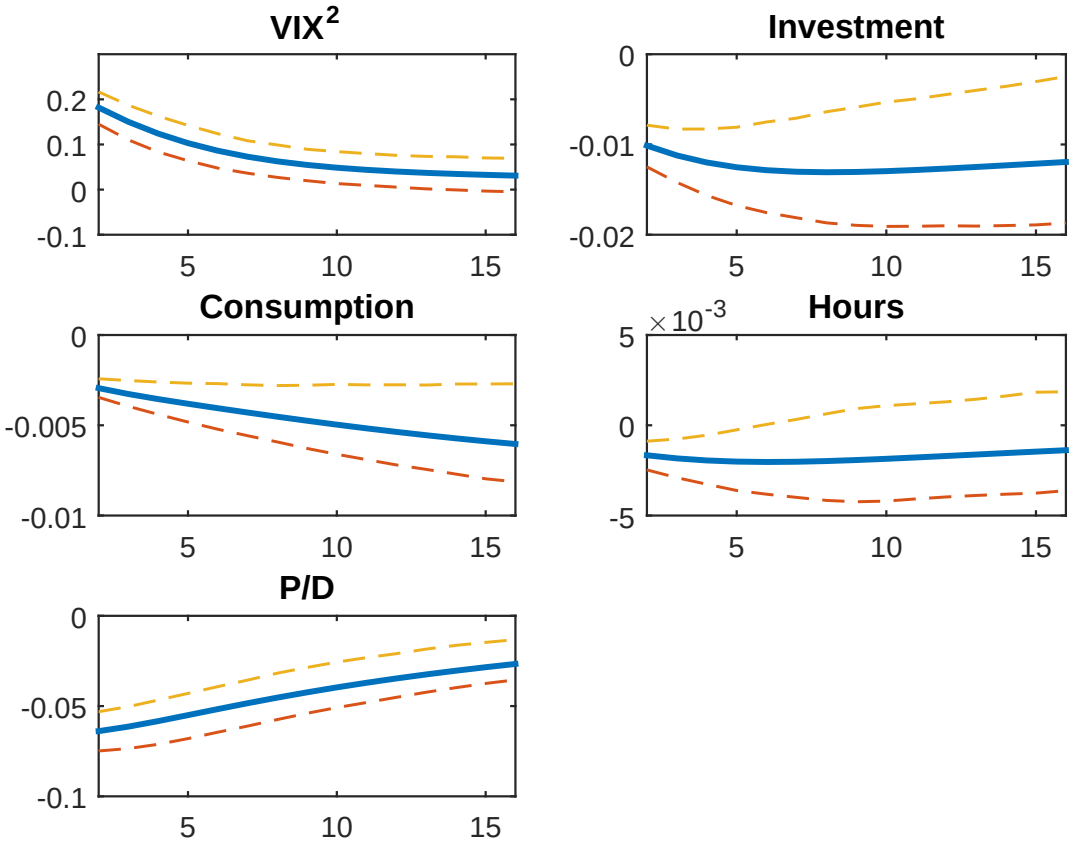

Notes: This figure plots the impulse response functions and the associated 68% error bands of several variables when there is a positive one-standard-deviation shock to the conditional volatility of productivity growth. The impulse responses are obtained by estimating a VAR model using the Bayesian approach developed by Sims and Zha (1998). The sample for estimation includes quarterly data from 1990:Q1 to 2016:Q1.

Figure 2: **Impulse responses: model AA3S**

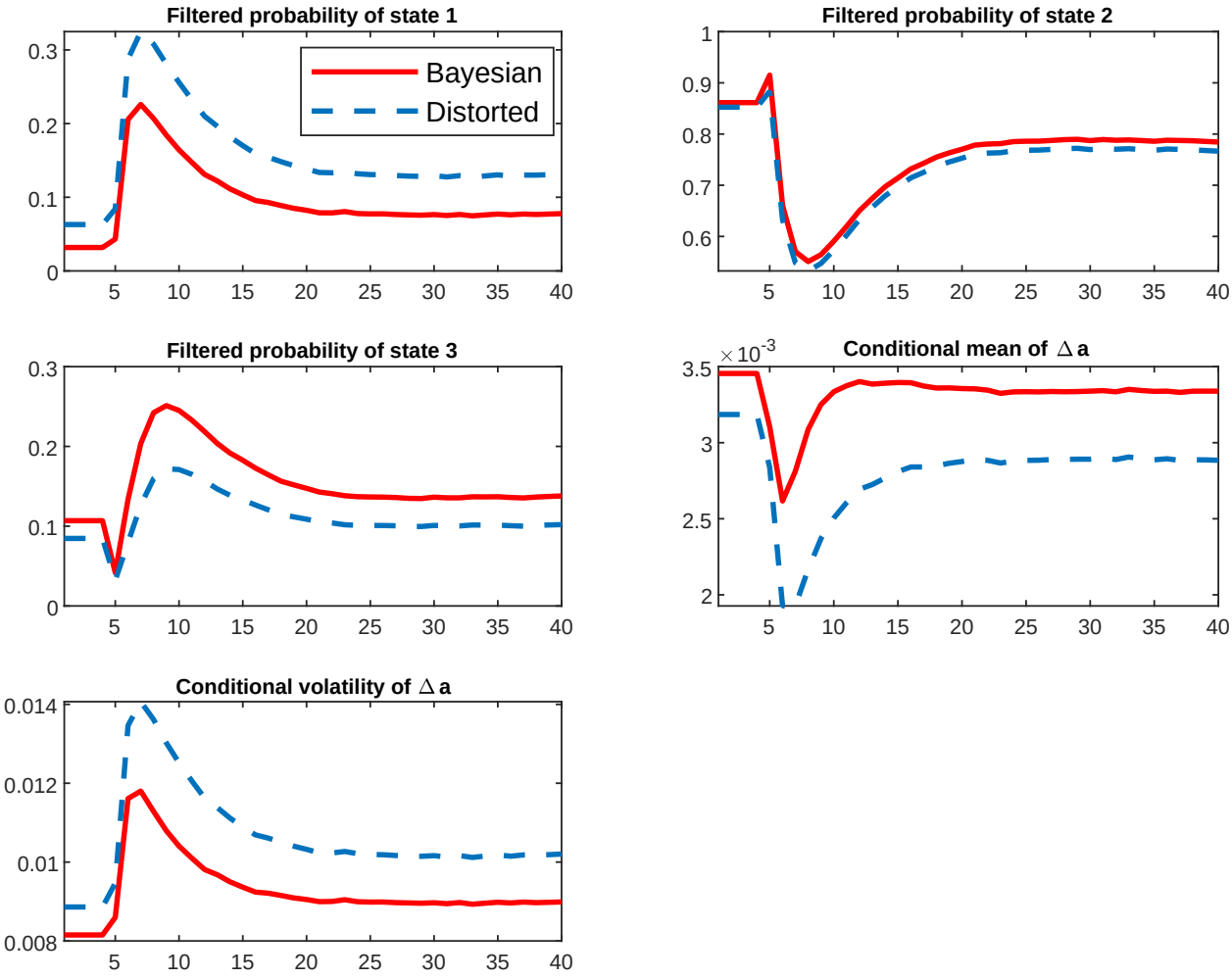

Notes: This figure plots the impulse response functions for the benchmark model AA3S when the economy switches from regime 2 to regime 1. The plots include filtered probabilities of the three states in the MS model and the conditional mean and volatility of productivity growth.

Figure 3: **Impulse responses: model AA3S**

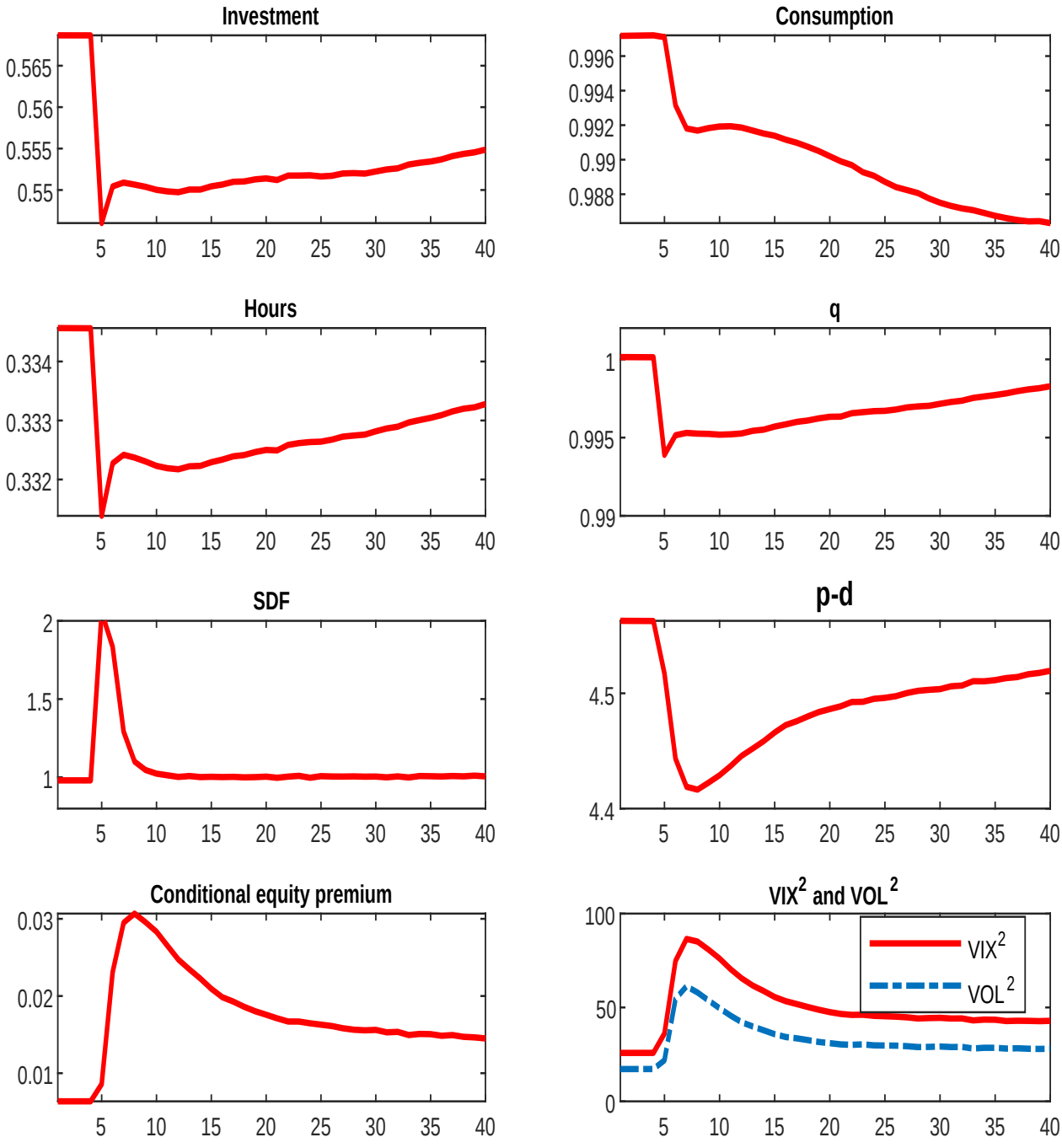

Notes: This figure plots the impulse response functions for the benchmark model AA3S when the economy switches from regime 2 to regime 1. The plots include macroeconomic quantities, asset prices and financial moments. The consumption and investment series are de-trended.

Figure 4: **VAR impulse responses**

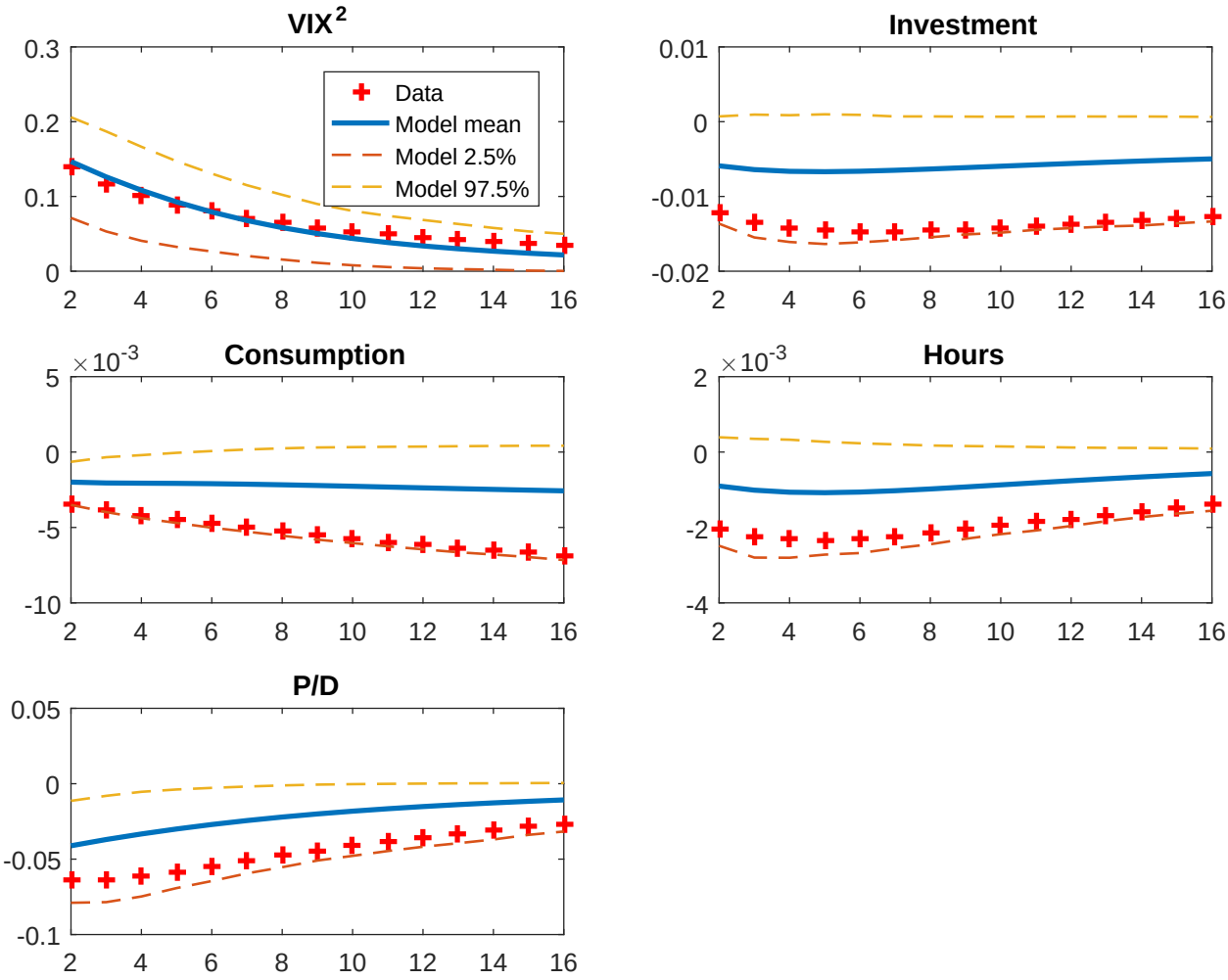

Notes: This figure plots the impulse response functions of several variables for the benchmark model AA3S when there is a positive one-standard-deviation shock to the conditional volatility of productivity growth. The impulse responses are obtained by estimating the Bayesian VAR model on 2,000 simulated samples. The plots show the mean impulse responses and the associated 2.5% and 97.5% ranges.

Figure 5: **Conditional moments**

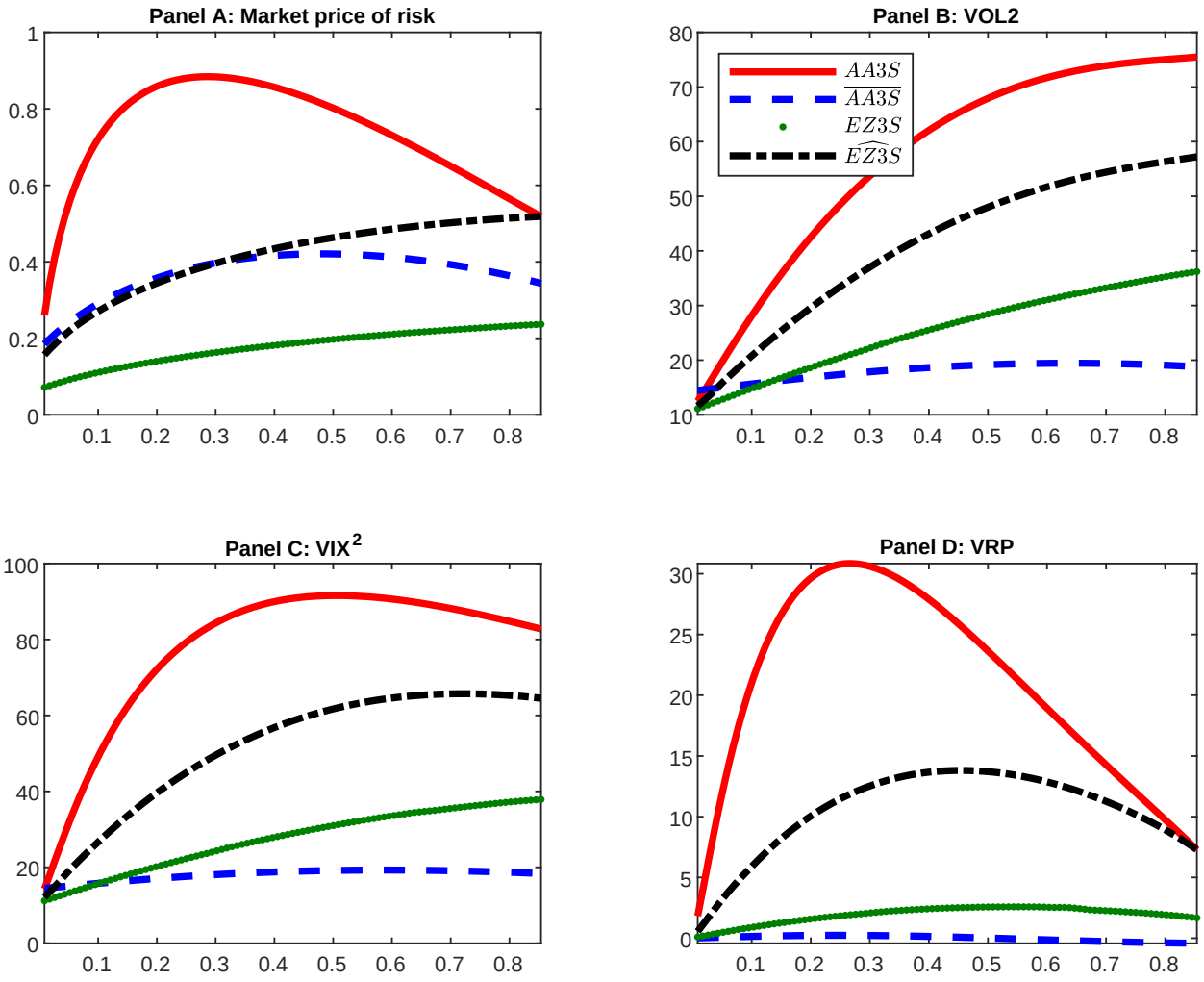

Notes: This figure plots conditional financial moments for models AA3S, $\overline{\text{AA3S}}$ and EZ3S. The filtered probability of regime 3 (the good regime) is assumed to remain at its steady-state level. The capital stock is set at its long run mean in the simulation. Conditional moments are plotted against the filtered probability of regime 1.

Figure 6: **The term structure of implied volatility**

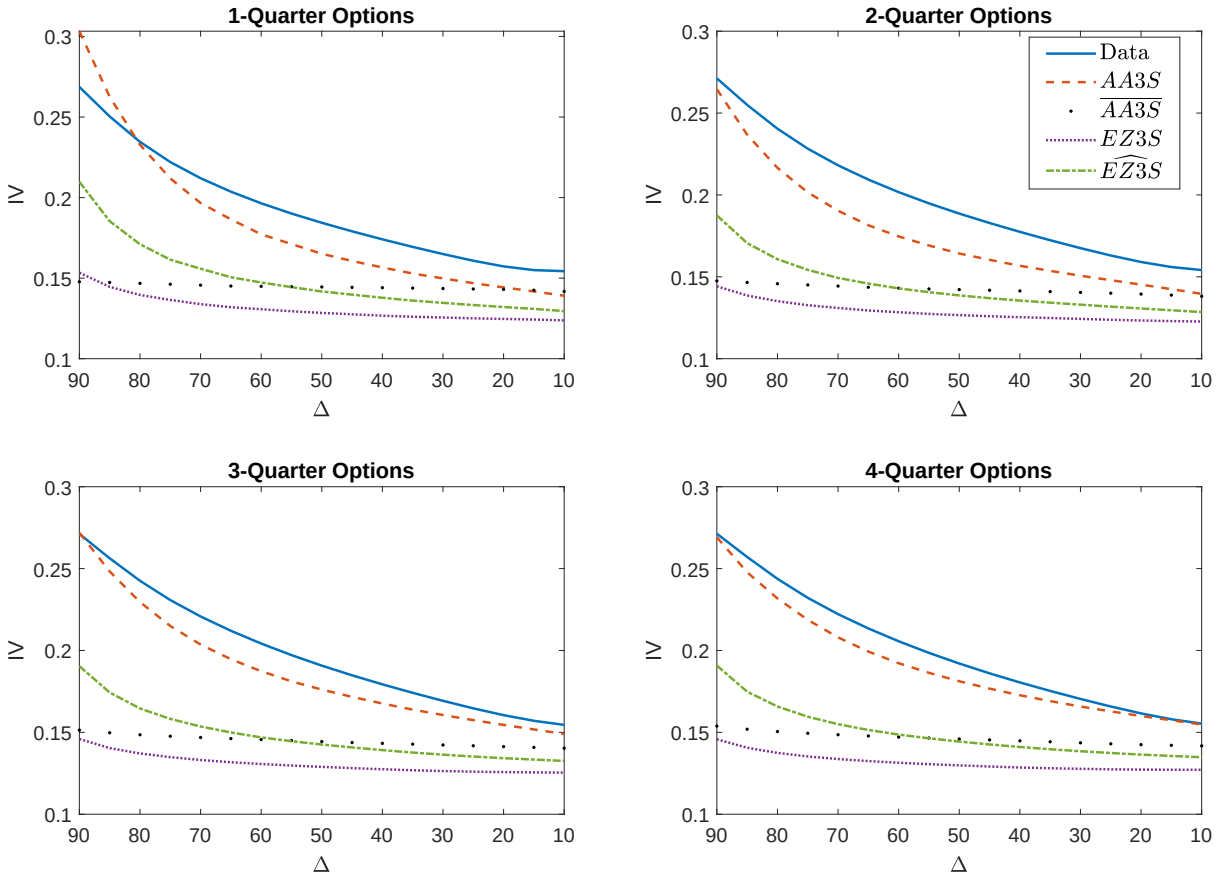

Notes: This figure plots the term structure of implied volatility (IV) of options across moneyness (measured by Black-Scholes call Δ) for the benchmark model AA3S, the $\overline{\text{AA3S}}$ model, the EZ3S model, the $\widehat{\text{EZ3S}}$ model, as well as the historical average skew in SPX options. The option maturities range from 1 to 4 quarters.

Figure 7: **Cross correlations with quantities and equity return**

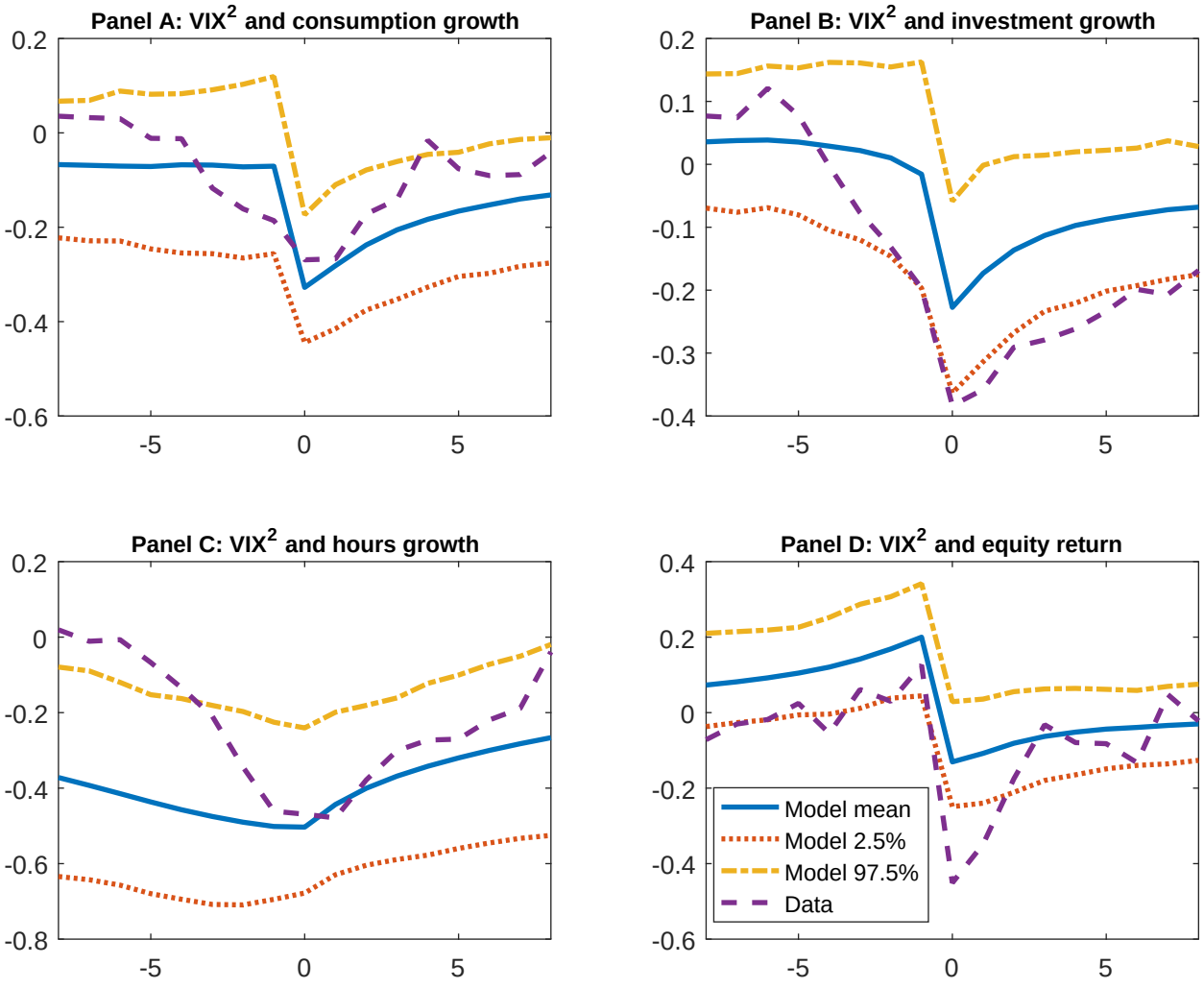

Notes: This figure plots the cross-correlograms between the risk-neutral variance and consumption growth, investment growth, hours growth, and the equity return (i.e., $Corr\left(VIX_t^2, x_{t+k}\right)$ for $k = -6$ to 6). The figure displays correlations for the historical data and the benchmark model AA3S. The cross-correlations are obtained on 2,000 simulated sample paths of the benchmark model. The plots show the mean cross-correlations and the associated 2.5% and 97.5% ranges. The historical data span quarterly data from 1990:Q1 to 2016:Q1.

Figure 8: **Cross correlations with volatilities of quantities and equity return**

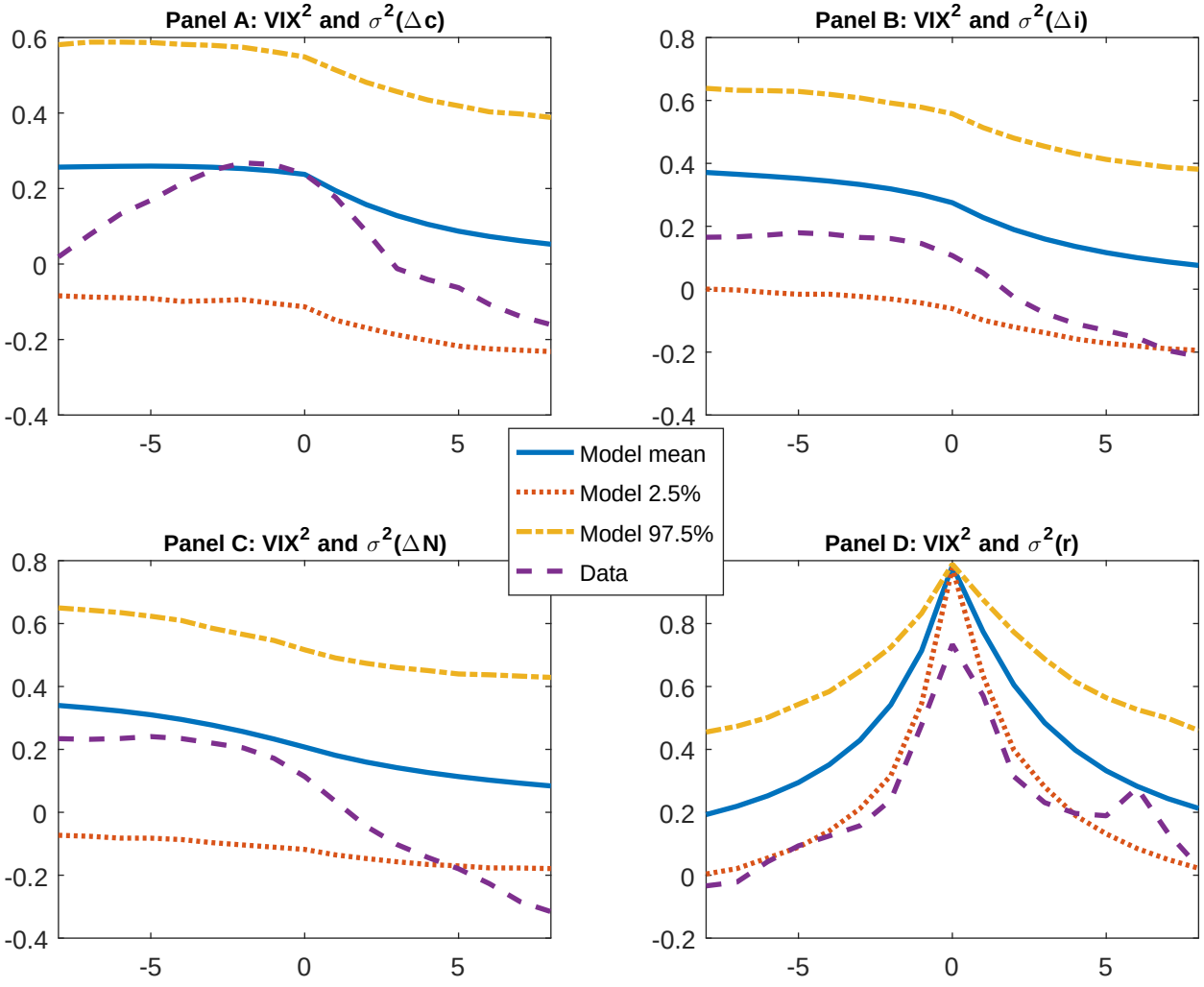

Notes: This figure plots the cross-correlograms between the risk-neutral variance and conditional volatilities of consumption growth, investment growth, and equity returns (i.e., $Corr\left(VIX_t^2, \sigma_{x,t+k}\right)$ for $k = -6$ to 6). The figure displays correlations for the historical data and the benchmark model AA3S. The cross-correlations are obtained on 2,000 simulated sample paths of the benchmark model. The plots show the mean cross-correlations and the associated 2.5% and 97.5% ranges. historical data span quarterly data from 1990:Q1 to 2016:Q1.

References

Abel, A. B., 1999. Risk premia and term premia in general equilibrium. Journal of Monetary Economics 43, 3–33.

Ai, H., 2010. Information quality and long-run risk: Asset pricing implications. Journal of Finance 65, 1333–1367.

Ai, H., Bansal, R., 2018. Risk preferences and the macroeconomic announcement premium. Econometrica 86, 1383–1430.

Altug, S., Collard, F., Çakmakli, C., Mukerji, S., Özsöylev, H., 2020. Ambiguous business cycles: A quantitative assessment. Review of Economic Dynamics forthcoming.

Anderson, E. W., Hansen, L. P., Sargent, T. J., 2003. A quartet of semigroups for model specification, robustness, price of risk, and model detection. Journal of the European Economic Association 1, 68–123.

Backus, D., Ferriere, A., Zin, S., 2015. Risk and ambiguity in models of business cycles. Journal of Monetary Economics 69, 42–63.

Bali, T. G., Zhou, H., 2016. Risk, uncertainty, and expected returns. Journal of Financial and Quantitative Analysis 51, 707–735.

Bansal, R., Yaron, A., 2004. Risks for the long run: A potential resolution of asset pricing puzzles. Journal of Finance 59, 1481–1509.

Bianchi, F., Ilut, C., Schneider, M., 2018. Uncertainty shocks, asset supply and pricing over the business cycle. Review of Economic Studies 85, 810–854.

Bloom, N., 2009. The impact of uncertainty shocks. Econometrica 77, 623–685.

Bloom, N., Floetotto, M., Jaimovich, N., Saporta-Eksten, I., Terry, S. J., 2018. Really uncertain business cycles. Econometrica 86, 1031–1065.

Bollerslev, T., Tauchen, G., Zhou, H., 2009. Expected stock returns and variance risk premia. Review of Financial Studies 22, 4463–4492.

Cagetti, M., Hansen, L. P., Sargent, T., Williams, N., 2002. Robustness and pricing with uncertain growth. Review of Financial Studies 15, 363–404.

Cecchetti, S. G., Lam, P.-S., Mark, N. C., 2000. Asset pricing with distorted beliefs: Are equity returns too good to be true? American Economic Review 90, 787–805.

Chen, H., Ju, N., Miao, J., 2014. Dynamic asset allocation with ambiguous return predictability. Review of Economic Dynamics 17, 799–823.

Chen, Z., Epstein, L. G., 2002. Ambiguity, risk and asset returns in continuous time. Econometrica 70, 1403–1443.

Cogley, T., Sargent, T. J., 2008. The market price of risk and the equity premium: A legacy of the great depression? Journal of Monetary Economics 55, 454–476.

Collard, F., Mukerji, S., Sheppard, K., Tallon, J.-M., 2018. Ambiguity and the historical equity premium. Quantitative Economics 9, 945–993.

Collin-Dufresne, P., Johannes, M., Lochstoer, L. A., 2016. Parameter learning in general equilibrium: The asset pricing implications. American Economic Review 106, 664–698.

Croce, M., Nguyen, T., Schmid, L., 2012. The market price of fiscal uncertainty. Journal of Monetary Economics 59, 401–416.

Croce, M. M., 2014. Long-run productivity risk: A new hope for production-based asset pricing? Journal of Monetary Economics 66, 13–31.

David, A., 1997. Fluctuating confidence in stock markets: Implications for returns and volatility. Journal of Financial and Quantitative Analysis 32, 427–462.

Dew-Becker, I., Giglio, S., Le, A., Rodriguez, M., 2017. The price of variance risk. Journal of Financial Economics 123, 225–250.

Drechsler, I., 2013. Uncertainty, time-varying fear, and asset prices. Journal of Finance 68, 1843–1889.

Drechsler, I., Yaron, A., 2011. What's vol got to do with it. Review of Financial Studies 24, 1–45.

Favilukis, J., Lin, X., 2015. Wage rigidity: A quantitative solution to several asset pricing puzzles. Review of Financial Studies 29, 148–192.

Gallant, A. R., Jahan-Parvar, M. R., Liu, H., 2019. Does smooth ambiguity matter for asset pricing? Review of Financial Studies 32, 3617–3666.

Gilboa, I., Schmeidler, D., 1989. Maxmin expected utility with non-unique priors. Journal of Mathematical Economics 18, 141–153.

Gourio, F., 2012. Disaster risk and business cycles. American Economic Review 102, 2734–2766.

Hamilton, J. D., 1990. Analysis of time series subject to changes in regimes. Journal of Econometrics 45, 39–70.

Hayashi, T., Miao, J., 2011. Intertemporal substitution and recursive smooth ambiguity preferences. Theoretical Economics 6, 423–472.

Hodrick, R., Prescott, E. C., 1997. Postwar U.S. business cycles: An empirical investigation. Journal of Money, Credit, and Banking 29, 1–16.

Ilut, C., Schneider, M., 2014. Ambiguous business cycles. American Economic Review 104, 2368–2399.

Jahan-Parvar, M., Liu, H., 2014. Ambiguity aversion and asset prices in production economies. Review of Financial Studies 27, 3060–3097.

Jermann, U. J., 1998. Asset pricing in production economies. Journal of Monetary Economics 41, 257–275.

Johannes, M., Lochstoer, L. A., Mou, Y., 2016. Learning about consumption dynamics. Journal of Finance 71, 551–600.

Ju, N., Miao, J., 2012. Ambiguity, learning, and asset returns. Econometrica 80, 559–591.

Kaltenbrunner, G., Lochstoer, L., 2010. Long-run risk through consumption smoothing. Review of Financial Studies 23 (8), 3190–3224.

Klibanoff, P., Marinacci, M., Mukerji, S., 2005. A smooth model of decision making under ambiguity. Econometrica 73, 1849–1892.

Klibanoff, P., Marinacci, M., Mukerji, S., 2009. Recursive smooth ambiguity preferences. Journal of Economic Theory 144, 930–976.

Kuehn, L.-A., Petrosky-Nadeau, N., Zhang, L., 2013. An equilibrium asset pricing model with labor market search. Working paper.

Leduc, S., Liu, Z., 2016. Uncertainty shocks are aggregate demand shocks. Journal of Monetary Economics 82, 20–35.

Li, Y., Yang, L., 2013. Asset pricing implications of dividend volatility. Management Science 59, 2036–2055.

Liu, H., Miao, J., 2015. Growth uncertainty, generalized disappointment aversion and production-based asset pricing. Journal of Monetary Economics 69, 70–89.

Mehra, R., Prescott, E. C., 1985. The equity premium: a puzzle. Journal of Monetary Economics 15, 145–161.

Miao, J., Wei, B., Zhou, H., 2018. Ambiguity aversion and variance premium. Quarterly Journal of Finance 9, 1–36.

Schorfheide, F., Song, D., Yaron, A., 2018. Identifying Long-Run Risks: A Bayesian Mixed-Frequency Approach. Econometrica 86, 617–654.

Sims, C. A., Zha, T., 1998. Bayesian methods for dynamic multivariate models. International Economic Review 39, 949–968.

Swanson, E. T., 2012. Risk aversion and the labor margin in dynamic equilibrium models. American Economic Review 102, 1663–1691.

Swanson, E. T., 2018. Risk aversion, risk premia, and the labor margin with generalized recursive preferences. Review of Economic Dynamics 28, 290–321.

Veronesi, P., 1999. Stock market overreaction to bad news in good times: A rational expectations equilibrium model. Review of Financial Studies 12, 975–1007.

Zhou, G., Zhu, Y., 2014. Macroeconomic volatilities and long-run risks of asset prices. Management Science 61, 413–430.

Zhou, H., 2018. Variance risk premia, asset predictability puzzles, and macroeconomic uncertainty. Annual Review of Financial Economics 10, 481–497.

Internet Appendix to "Financial Uncertainty with Ambiguity and Learning"

Hening Liu* Yuzhao Zhang†

Alliance Manchester Business School
The University of Manchester

Rutgers Business School
Rutgers University

September 2020

A: Numerical algorithm

The equilibrium can be characterized by the social planner's problem. This economy can be decentralized using this standard arguments: the representative household supplies labor inputs and trades shares issued by the firm and risk-free bonds, and the firm chooses labor and investment to maximize its firm value (i.e., the discounted present value of future cash flows). The social planner's problem is to choose $\{C_t, I_t, N_t\}$ to maximize the generalized recursive smooth ambiguity utility function, subject to the resource constraint $Y_t = C_t + I_t$ and the law of motion for capital accumulation. In the model, the state variables are $\{K_t, A_t, \boldsymbol{\pi}_t\}$. Denote $J_t = J(K_t, A_t, \boldsymbol{\pi}_t)$, the value function. The Bellman equation can be written as

$$J_t = \max_{C_t, I_t, N_t} \left[(1-\beta) U_t^{1-\frac{1}{\psi}} + \beta \left(\mathbb{E}_{\boldsymbol{\pi}_t} \left[\left(\mathbb{E}_{\{s_{t+1}, t\}} \left[J_{t+1}^{1-\gamma} \right] \right)^{\frac{1-\eta}{1-\gamma}} \right] \right)^{\frac{1-\frac{1}{\psi}}{1-\eta}} \right]^{\frac{1}{1-\frac{1}{\psi}}}$$

*Alliance Manchester Business School, The University of Manchester, Booth Street West, Manchester M15 6PB, UK. e-mail: hening.liu@manchester.ac.uk.

†Rutgers Business School, Rutgers, The State University of New Jersey; Newark, NJ, 07102, USA. e-mail: yzhang@business.rutgers.edu.

Due to homogeneity and the fact that K_t, C_t, I_t and Y_t share the common trend A_t, we can write:

$$\left\{\tilde{K}_t, \tilde{C}_t, \tilde{I}_t, \tilde{Y}_t, \right\} = \left\{\frac{K_t}{A_t}, \frac{C_t}{A_t}, \frac{I_t}{A_t}, \frac{Y_t}{A_t}\right\}.$$

It follows that the value function can be rewritten as,

$$J\left(K_t, A_t, \boldsymbol{\pi}_t\right) = A_t \tilde{J}\left(\tilde{K}_t, \boldsymbol{\pi}_t\right)$$

for which $\tilde{J}\left(\tilde{K}_t, \boldsymbol{\pi}_t\right)$ satisfies the Bellman equation:

$$\tilde{J}_t = \max_{\tilde{C}_t, \tilde{I}_t, N_t} \left[(1-\beta)\left(\tilde{C}_t\left(1-N_t\right)^{\nu}\right)^{1-\frac{1}{\psi}} + \beta\left(\mathbb{E}_{\boldsymbol{\pi}_t}\left[\left(\mathbb{E}_{\{s_{t+1},t\}}\left[\left(\exp\left(\Delta a_{t+1}\right)\tilde{J}_{t+1}\right)^{1-\gamma}\right]\right)^{\frac{1-\eta}{1-\gamma}}\right]\right)^{\frac{1-\frac{1}{\psi}}{1-\eta}}\right]^{\frac{1}{1-\frac{1}{\psi}}}$$

subject to

$$\begin{aligned}
\tilde{C}_t + \tilde{I}_t &= \tilde{K}_t^{\alpha} N_t^{1-\alpha} \\
e^{\Delta a_{t+1}} \tilde{K}_{t+1} &= \left(1-\delta\right)\tilde{K}_t + \phi\left(\frac{\tilde{I}_t}{\tilde{K}_t}\right)\tilde{K}_t \\
\Delta a_t &= \mu\left(s_t\right) + \sigma\left(s_t\right)\epsilon_t, \quad \epsilon_t \sim N\left(0,1\right).
\end{aligned}$$

Because the model is nonlinear, the standard perturbation method is not applicable. We use the value function iteration method to solve the model numerically. The numerical algorithm proceeds as follows:

1. We compute the de-trended capital $\tilde{K}_{ss}$ in the deterministic steady state, assuming that the productivity growth rate is constant and equal to the steady-state level implied by the Markov-switching model. The state space for $\tilde{K}$ is set at $\left[\tilde{K}_{\min}, \tilde{K}_{\max}\right] = \left[0.2\tilde{K}_{ss}, 2.0\tilde{K}_{ss}\right]$. The capital grid has n_k grid points on this interval; these grid points are determined from Chebyshev zeros. We use $n_k = 100$ in the numerical computation. Further increasing n_k does not lead to significantly different results.

2. We construct the grid for the state belief vector $\boldsymbol{\pi}$ in a similar way. Each state variable in the belief vector has n_π grid points on the interval $[0,1]$. These grid points are determined

from Chebyshev zeros. For example, in the model with two regimes, $\boldsymbol{\pi} = \left\{\pi^1, \pi^2\right\}$ for $s = 1$ and 2 respectively, and we discretize a grid for π^1 only. In the model with three regimes, $\boldsymbol{\pi} = \left\{\pi^1, \pi^2, \pi^3\right\}$ for $s = 1$, 2 and 3 respectively, and we discretize grids for π^1 and π^2. We use $n_\pi = 40$ for discretizing each element in the belief vector. Further increasing n_π does not improve results.

3. We choose a grid for $\tilde{I}$. For each capital grid point, we construct equidistant points for $\tilde{I}$ bounded between 0 and $\tilde{K}^\alpha$. We use 100 pints for the $\tilde{I}$ grid.

4. We compute for each $(\tilde{K},\, \tilde{I})$ on the grid the value $N\left(\tilde{K}, \tilde{I}\right)$ that solves

$$\max_N \left(\tilde{K}^\alpha N^{1-\alpha} - \tilde{I}\right)(1-N)^\nu$$

   For each $\tilde{K}$ point, we apply an interpolation method to interpolate $N\left(\tilde{K}, \tilde{I}\right)$ onto the grid for $\tilde{I}$ and to obtain the interpolation coefficients.

5. We use Gauss-Hermite quadrature with 9 nodes to compute expectations with respect to conditional Gaussian densities of Δa.

6. For the two-regime model, our goal is to compute $\tilde{J}\left(\tilde{K}, \pi^1\right)$ on the grid $\left[\tilde{K}_{\min}, \tilde{K}_{\max}\right] \times \left[\pi^1_{\min}, \pi^1_{\max}\right]$. For the three-regime model, our goal is to compute $\tilde{J}\left(\tilde{K}, \pi^1, \pi^2\right)$ on the grid $\left[\tilde{K}_{\min}, \tilde{K}_{\max}\right] \times \left[\pi^1_{\min}, \pi^1_{\max}\right] \times \left[\pi^2_{\min}, \pi^2_{\max}\right]$. In this case, we only consider those combinations of π^1 and π^2 that yield appropriate conditional probabilities of the three regimes.

   The value function $\tilde{J}\left(\tilde{K}, \pi^1\right)$ is approximated by a set of Chebyshev coefficients multiplying product Chebyshev polynomials in $\tilde{K}$ and π^1. The value function $\tilde{J}\left(\tilde{K}, \pi^1, \pi^2\right)$ is approximated by a set of Chebyshev coefficients multiplying product Chebyshev polynomials in $\tilde{K}$, π^1 and π^2.

7. For the two-regime model, we denote the current period value function and the next period value function by:

$$\begin{aligned} \tilde{J} &= \tilde{J}\left(\tilde{K}, \pi^1\right) \\ \tilde{J}' &= \tilde{J}\left(\tilde{K}', \left(\pi^1\right)'\right) \end{aligned}$$

Given the current state $\left(\tilde{K}, \pi\right)$, we use a numerical optimizer to solve the social planner's problem:

$$\tilde{J} = \max_{\tilde{I},N} \left[(1-\beta)\tilde{U}^{1-\frac{1}{\psi}} + \beta \left(\mathbb{E}_{\pi^1} \left[\left(\mathbb{E}_{\{s'\}} \left[\left(\exp\left(\Delta a'\right) \tilde{J}' \right)^{1-\gamma} \right] \right)^{\frac{1-\eta}{1-\gamma}} \right] \right)^{\frac{1-\frac{1}{\psi}}{1-\eta}} \right]^{\frac{1}{1-\frac{1}{\psi}}}$$

for which

$$\tilde{U} = \left(\tilde{K}^{\alpha} N^{1-\alpha} - \tilde{I} \right) (1-N)^{\nu}.$$

The next period's state belief $\left(\pi^1\right)'$ is updated from π^1 given the next period's contingent growth rate $\Delta a'$. For $\left(\tilde{K}', \left(\pi^1\right)'\right)$ outside the grid points, we use a Chebyshev approximation to compute the value function. For a given investment policy $\tilde{I}$, we use the B-spline method to compute the corresponding optimal N.

8. For the three-regime model, we denote the current period value function and the next period value function by:

$$\begin{aligned} \tilde{J} &= \tilde{J}\left(\tilde{K}, \pi^1, \pi^2\right) \\ \tilde{J}' &= \tilde{J}\left(\tilde{K}', \left(\pi^1\right)', \left(\pi^2\right)'\right) \end{aligned}$$

The social planner's problem is

$$\tilde{J} = \max_{\tilde{I},N} \left[(1-\beta)\tilde{U}^{1-\frac{1}{\psi}} + \beta \left(\mathbb{E}_{\{\pi^1,\pi^2\}} \left[\left(\mathbb{E}_{\{s'\}} \left[\left(\exp\left(\Delta a'\right) \tilde{J}' \right)^{1-\gamma} \right] \right)^{\frac{1-\eta}{1-\gamma}} \right] \right)^{\frac{1-\frac{1}{\psi}}{1-\eta}} \right]^{\frac{1}{1-\frac{1}{\psi}}}$$

9. $\tilde{J}^*$ denotes the updated value function on each grid in the state space after an iteration. The algorithm then returns to the previous step. The stopping rule is that the new value function and the old value function satisfies $\left|\tilde{J}^* - \tilde{J}\right| / \left|\tilde{J}\right| < 10^{-12}$.

10. The pricing kernel can be rewritten as,

$$M_{t,t+1} = \beta \left(\frac{\tilde{C}_{t+1}}{\tilde{C}_t} e^{\Delta a_{t+1}} \right)^{-\frac{1}{\psi}} \left(\frac{1-N_{t+1}}{1-N_t} \right)^{\left(1-\frac{1}{\psi}\right)\nu} \left(\frac{\tilde{J}_{t+1} e^{\Delta a_{t+1}}}{\mathcal{R}_t \left(\tilde{J}_{t+1} e^{\Delta a_{t+1}} \right)} \right)^{\frac{1}{\psi}-\gamma} \left(\frac{\left(\mathbb{E}_{s_{t+1},t} \left[\tilde{J}_{t+1}^{1-\gamma} e^{(1-\gamma)\Delta a_{t+1}} \right] \right)^{\frac{1}{1-\gamma}}}{\mathcal{R}_t \left(\tilde{J}_{t+1} e^{\Delta a_{t+1}} \right)} \right)^{-(\eta-\gamma)}$$

To compute the pricing kernel, we use interpolation (B-spline and linear) methods to compute policy functions $N\left(\tilde{K}, \boldsymbol{\pi}\right)$ and $\tilde{I}\left(\tilde{K}, \boldsymbol{\pi}\right)$. For the three-regime model, we use three-dimensional linear interpolation to compute policy functions.

11. The price-dividend ratio $\frac{P_t}{D_t} = \xi\left(\tilde{K}_t, \boldsymbol{\pi}_t\right)$ satisfies the Euler equation

$$\xi\left(\tilde{K}_t, \boldsymbol{\pi}_t\right) = \mathbb{E}_t \left[M_{t,t+1} \left(1 + \xi\left(\tilde{K}_{t+1}, \boldsymbol{\pi}_{t+1}\right) \right) \exp\left(\Delta d_{t+1}\right) \right]$$

We use linear interpolation methods to find the fixed point to the functional equation above. Our computer code is written in Fortran OpenMP with parallel programming.

B: Calibrating ambiguity aversion

B1: Detection-error probabilities

To compute the detection-error probability, we need to simulate data from both the reference model and distorted model. Suppose that the reference model is the three-regime Markov-switching model

$$\Delta a_t = \mu\left(s_t\right) + \sigma\left(s_t\right)\epsilon_t, \quad \epsilon_t \sim N\left(0,1\right)$$

where $s_t = 1, 2$ or 3. State s_t follows a Markov chain with the transition probabilities matrix

$$\boldsymbol{P} = \begin{bmatrix} p_{11} & p_{12} & p_{13} \\ p_{21} & p_{22} & p_{23} \\ p_{31} & p_{32} & p_{33} \end{bmatrix}$$

where $p_{ij} = \Pr(s_t = j | s_{t-1} = i)$ and

$$\begin{aligned} p_{12} &= 1 - p_{11} - p_{13} \\ p_{23} &= 1 - p_{21} - p_{22} \\ p_{32} &= 1 - p_{31} - p_{33}. \end{aligned}$$

To determine how ambiguity aversion distorts the reference model, we consider the following problem:

$$\tilde{J}_t = \max_{\tilde{C}_t, \tilde{I}_t, N_t} \left[(1-\beta) \left(\tilde{C}_t (1-N_t)^{\nu} \right)^{1-\frac{1}{\psi}} + \beta \left(\mathbb{E}_{s_t} \left[\left(\mathbb{E}_{\{s_{t+1},t\}} \left[\left(\exp(\Delta a_{t+1}) \tilde{J}_{t+1} \right)^{1-\gamma} \right] \right)^{\frac{1-\eta}{1-\gamma}} \right] \right)^{\frac{1-\frac{1}{\psi}}{1-\eta}} \right]^{\frac{1}{1-\frac{1}{\psi}}}$$

where

$$\tilde{J}_t \equiv \tilde{J}\left(\tilde{K}_t, s_t\right) = J(K_t, A_t, s_t) A_t^{-1}.$$

The corresponding SDF for this problem is

$$\hat{M}_{t,t+1} = \hat{M}^{EZ}_{t,t+1} \hat{M}^{AA}_{s_{t+1},t}$$

with

$$\hat{M}^{EZ}_{t,t+1} = \beta \left(\frac{C_{t+1}}{C_t} \right)^{-\frac{1}{\psi}} \left(\frac{1-N_{t+1}}{1-N_t} \right)^{\left(1-\frac{1}{\psi}\right)\nu} \left(\frac{J_{t+1}}{\mathcal{R}_t(J_{t+1})} \right)^{\frac{1}{\psi}-\gamma}$$

and

$$\hat{M}^{AA}_{s_{t+1},t} = \left(\frac{\left(\mathbb{E}_{\{s_{t+1},t\}} \left[J_{t+1}^{1-\gamma} \right] \right)^{\frac{1}{1-\gamma}}}{\mathcal{R}_t(J_{t+1})} \right)^{-(\eta-\gamma)}$$

where

$$\mathcal{R}_t(J_{t+1}) = \left(\mathbb{E}_{s_t} \left[\left(\mathbb{E}_{\{s_{t+1},t\}} \left[J_{t+1}^{1-\gamma} \right] \right)^{\frac{1-\eta}{1-\gamma}} \right] \right)^{\frac{1}{1-\eta}}.$$

It can be shown that the distorted model has the transition probabilities

$$\tilde{p}_{ij,t} = \frac{p_{ij}\left(\mathbb{E}_{\{s_{t+1}=j,t\}}\left[J_{t+1}^{1-\gamma}\right]\right)^{-\frac{\eta-\gamma}{1-\gamma}}}{\sum_{j=1}^{3} p_{ij}\left(\mathbb{E}_{\{s_{t+1}=j,t\}}\left[J_{t+1}^{1-\gamma}\right]\right)^{-\frac{\eta-\gamma}{1-\gamma}}},\ i = 1, 2 \text{ and } 3$$

i.e., ambiguity aversion distorts the transition probabilities for the growth regimes. The numerical algorithm of approximating detection-error probabilities is described in the following steps.

1. Simulate Markov states $\{s_t\}_{t=1}^{T}$ and growth rates $\{\Delta a_t\}_{t=1}^{T}$ under the reference model with the objective transition probabilities in matrix $\boldsymbol{P}$.

2. Assume that s_t is unobservable. Obtain filtered probabilities ($\boldsymbol{\pi}_t$) of state s_t according to Bayes' rule.

3. Solve the model and simulate $\mathbb{E}_{\{s_{t+1}=j,t\}}\left[J_{t+1}^{1-\gamma}\right]$, $j = 1, 2$ and 3. Compute distorted transition probabilities and obtain filtered probabilities of s_t given the distorted transition probabilities.

4. Compute the log likelihood function under the reference model:

$$\ln L_T^r = \sum_{t=1}^{T} \ln\left\{\sum_{s_t} f\left(\Delta a_t | s_t\right) \Pr\left(s_t | \mathcal{F}_{t-1}\right)\right\}$$

   where $f\left(\Delta a_t | s_t\right)$ is conditional likelihood, and $\Pr\left(s_t | \mathcal{F}_{t-1}\right)$ is the filtered probability of state s_t.

5. Compute the log likelihood function under the distorted model:

$$\ln L_T^d = \sum_{t=1}^{T} \ln\left\{\sum_{s_t} f\left(\Delta a_t | s_t\right) \widetilde{\Pr\left(s_t | \mathcal{F}_{t-1}\right)}\right\}$$

   where $\widetilde{\Pr\left((s_t^{\mu}, s_t^{\sigma}) | \mathcal{F}_{t-1}\right)}$ is the filtered probability by applying the distorted transition probabilities in Bayes' rule. The fraction of simulations for which $\ln\left(\frac{L_T^d}{L_T^r}\right) > 0$ approximates the probability that the distorted model generated the data, while the data are actually generated by the reference model. This fraction is denoted by p_r.

6. Perform a symmetrical computation and start by simulating states $\{s_t\}_{t=1}^{T}$, assuming that

the Markov chain is governed by distorted transition probabilities $\tilde{p}_{ij,t}$. Simulate $\{\Delta a_t\}_{t=1}^T$ accordingly from the distorted model.

7. For a simulation $\{\Delta a_t\}_{t=1}^T$, apply the Bayes' rule to compute filtered probabilities of s_t using the distorted transition probabilities. Compute the log likelihood function under the distorted model when the data are generated from that model. Apply the Bayes' rule to compute filtered probabilities using the objective transition probabilities and compute the log likelihood function under the reference model. The fraction of simulations for which $\ln\left(\frac{L_T^r}{L_T^d}\right) > 0$ fraction approximates the probability that the reference model generated the data when the data are actually drawn from the distorted model. This fraction is denoted by p_d.

   Following Anderson et al. (2003), we assume the same prior on the reference and the distorted models, and the detection-error probability is defined by,

$$p(\eta) = \frac{1}{2}(p_r + p_d).$$

   The length of the simulation is set at $T = 200$ quarters. The number of simulations is set at $N = 20,000$.

B2: Thought experiments

Following Halevy (2007) and Ju and Miao (2012), we use thought experiments — similar to the Ellsberg Paradox — as an an alternative way to calibrate the degree of ambiguity aversion. We consider the classic example of the Ellsberg Paradox with two urns. Suppose that the two urns contain black and white balls. Subjects know that the first urn has 50 white and 50 black balls, and the other ambiguous urn has 100 balls, either white or black. The exact numbers of the two colors in the ambiguous urn are unknown to the subjects. Subjects are told to bet on the color of a ball drawn from each urn, and they will win a prize worth d dollars if a bet on a specific urn is correct; otherwise, they win nothing and are not penalized. Halevy (2007) reports that the majority of subjects prefer a bet on the first urn over the second urn.

Expected utility fails to explain this behavior, independent of risk aversion or the subjects' beliefs. This is because under expected utility, the certainty equivalents of a bet are identical for

the two urns. However, ambiguity aversion can create a difference between the certainty equivalents across the two urns, leading to "ambiguity premium". As in Ju and Miao (2012), ambiguity premium is defined as,

$$u^{-1}\left(\int_{\Theta}\int_{S}u(c)d\theta d\zeta\left(\theta\right)\right)-v^{-1}\left(\int_{\Theta}v\left(u^{-1}\left(\int_{S}u\left(c\right)d\theta\right)\right)d\zeta\left(\theta\right)\right).$$

For the utility function we consider in the paper, the functional forms of u and v are given by:

$$\begin{aligned} u\left(c\right) &= \frac{c^{1-\gamma}}{1-\gamma},\gamma>0,\neq 1 \\ v\left(x\right) &= \frac{x^{1-\eta}}{1-\eta},\eta>0,\neq 1. \end{aligned}$$

Ju and Miao (2012) specify the set of probability distributions for the bet on the second urn as (0,1) and (1,0), i.e., $\Theta=\{(0,1),(1,0)\}$, and the subjective prior as $\zeta=(0.5,0.5)$. Also, the wealth level is denoted by w. Then, ambiguity premium is defined as,

$$\left(0.5(d+w)^{1-\gamma}+0.5w^{1-\gamma}\right)^{\frac{1}{1-\gamma}}-\left(0.5(d+w)^{1-\eta}+0.5w^{1-\eta}\right)^{\frac{1}{1-\eta}}.$$

for $\eta>\gamma$. The ambiguity premium depends on the prize-wealth ratio d/w. Table B1 shows the ambiguity premium, expressed as a percentage of the expected value of the bet $d/2$, for various parameter values of η and risk aversion set at $\gamma=5$. Because researchers often use small bets in experimental studies, we consider three different prize-wealth ratios: $d/w=1.5\%$, $d/w=1\%$, and $d/w=0.75\%$. All else being equal, a smaller bet implies a lower ambiguity premium. Given previous experimental evidence documented by Camerer (1999) and Halevy (2007), the ambiguity premium is typically about 10-20 percent of the expected value of a bet. Consistent with this finding, the value of the ambiguity aversion parameter used in our calibration ($\eta=55$) is reasonable.

C: Data on productivity

To construct aggregate productivity data, we follow the methodology adopted by Stock and Watson (1999) and use data from the National Income and Product Accounts (NIPA). Quarterly data on Solow residuals are constructed from non-farm gross domestic product (GDP) (Table 1.3.6, line

Table B1: **Ambiguity premium**

η	10	20	30	40	50	60
Prize-wealth ratio=1.5%	0.019	0.056	0.092	0.128	0.163	0.198
Prize-wealth ratio=1%	0.012	0.037	0.062	0.086	0.111	0.135
Prize-wealth ratio=0.75%	0.009	0.028	0.047	0.065	0.084	0.102

This table reports the ambiguity premium, expressed as a percentage of the expected value of the bet $d/2$, for various values of η. The risk aversion parameter γ is set at 5.

3), quarterly capital stock, and labor (hours of nonfarm employees). Quarterly capital values are constructed from interpolating annual non-residential capital stock (Fixed Assets Table 1.1, line 4) deflated by the price index for non-residential investment (Table 1.1.4, line 9) using quarterly non-residential fixed investment (Table 1.1.5, line 9) deflated by the corresponding price deflator. The capital share α is assumed to be 0.36. The Solow residuals are rescaled by $1-\alpha$ to obtain labor-augmenting technology level A_t.

D: Additional Results

D1: Model calibration: two-state Markov-switching model

Parameter estimates of the two-state Markov-switching model are reported in Table D1. In the Internet Appendix, we use these parameter values as the basis for the model calibration. The numerical algorithm of solving the two-regime model has been illustrated in Section A. Other parameter choices remain the same as in the benchmark model AA3S in the main paper. For model AA2S, we choose $\eta = 40$ to match equity premium in the data. This procedure yields $\mathbb{E}(VRP) = 5.02$ for the model, which is less than half of the data moment. Other model implied moments of VRP are not in line with the corresponding moments in the data. We provide three alternative models for comparison, EZ2S ($\gamma = 5$, no ambiguity aversion), $\widehat{\text{EZ2S}}$ ($\gamma = 10$, no ambiguity aversion), and $\overline{\text{AA2S}}$ (no time-varying volatility).

Table D1: **Parameter Estimates of the Two-state Markov-switching Model**

$$\Delta a_t = \mu(s_t) + \sigma(s_t)\epsilon_t, \quad \epsilon_t \sim N(0,1),$$

μ_1	μ_2	σ_1	σ_2	p_{11}	p_{22}
-0.989	1.026	3.726	1.007	0.753	0.977
(0.100)	(0.112)	(1.320)	(0.140)	(0.003)	(0.037)

This table reports the maximum likelihood estimates of parameters in the Markov-switching model with two regimes. Data for estimation are quarterly total factor productivity growth rates from 1947:Q1 to 2016:Q1. Standard errors are reported in parentheses.

D2: Financial leverage

We introduce financial leverage using the approach of Jermann (1998) and assume that Modigliani and Miller's Theorem holds such that the equilibrium allocation and firm value are unaffected by capital structure. We do not consider corporate taxes or default. Financial leverage is introduced by assuming that in each period, the firm issues long-term discount bonds with the value given by a fixed proportion (ω) of the capital stock K_t. Specifically, if the price of the n-period discount bonds is denoted by $B_t^{(n)}$, the dividend payout is

$$\tilde{D}_t = Y_t - w_t N_t - I_t + \omega K_t - \frac{\omega K_{t-n}}{B_{t-n}^{(n)}}$$

where ωK_t is the proceeds from the bond issuance and $\omega K_{t-n}/B_{t-n}^{(n)}$ is the repayment to the debt holders who have purchased the n-period discount bonds in period $t-n$. The no-arbitrage condition implies that bond prices satisfy the equation

$$B_t^{(n)} = \mathbb{E}_t\left[M_{t+1}B_{t+1}^{(n-1)}\right], \quad B_t^{(0)} = 1 \ \forall t$$

The debt value is equal to the total market value of all outstanding bonds from period $t-n+1$ to period t:

$$DV_t = \sum_{j=1}^{n} \frac{\omega K_{t-n+j}}{B_{t-n+j}^{(n)}} B_t^{(j)}$$

Table D2: **Calibration: Models with the Two-regime MS Process**

	$\sigma_{\Delta c}(\%)$	$\sigma_{\Delta i}(\%)$	$\sigma_{\Delta y}(\%)$	$\rho(\Delta i, \Delta y)$	$\rho(\Delta c, \Delta y)$	$\rho(\Delta c, \Delta i)$
AA2S	0.80	4.17	1.96	0.98	0.85	0.75
EZ2S	1.07	4.36	1.94	0.94	0.58	0.29
$\widehat{\text{EZ2S}}$	0.89	3.98	1.90	0.97	0.87	0.76
$\overline{\text{AA2S}}$	0.86	3.09	1.59	0.96	0.81	0.63

	$\mathbb{E}(R - R_f)(\%)$	$\sigma(R - R_f)(\%)$	$\mathbb{E}(VRP)$	$\sigma(VRP)$	Skewness (VRP)	Kurtosis (VRP)
AA2S	6.04	14.22	5.02	2.47	2.09	6.95
EZ2S	4.40	12.05	0.89	0.11	-1.12	3.84
$\widehat{\text{EZ2S}}$	8.15	13.03	3.57	0.93	1.37	3.53
$\overline{\text{AA2S}}$	0.74	12.05	0.06	0.05	2.63	11.43

This table reports unconditional moments for models with the two-regime Markov-switching process of productivity growth. Model AA2S assumes $\eta = 40$. Model $\overline{\text{AA2S}}$ differs from AA2S in that the innovation shock to productivity growth has constant volatility ($\sigma(s_t) = \sigma$). Model EZ2S features ambiguity neutrality ($\gamma = \eta = 5$). Model $\widehat{\text{EZ2S}}$ features ambiguity neutrality with a high risk aversion ($\gamma = \eta = 10$). The results are based on 2,000 simulations, and each simulation contains 400 quarters of data.

where $\omega K_{t-n+j}/B^{(n)}_{t-n+j}$ represents the amount of bond issuance in period $t - n + j$. The market value of firm is given by $FV_t = q_t K_{t+1}$. Thus, equity value is $P^E_t = FV_t - DV_t$, and the return on equity is

$$R^E_t = \frac{P^E_t + \tilde{D}_t}{P^E_{t-1}}$$

We then compute VOL^2_t and VIX^2_t based on the equity return defined above. We simulate 2,000 sample paths, where each sample path contains 400 quarters of data. Moments of excess returns and VRP are shown in the table below.

Table D3: **Financial moments**

	$\mathbb{E}(R - R_f)(\%)$	$\sigma(R - R_f)(\%)$	$\mathbb{E}(VRP)$	$\sigma(VRP)$	Skewness (VRP)	Kurtosis (VRP)
AA3S_{lev}	1.77	3.86	1.05	1.84	5.61	42.95
EZ3S_{lev}	0.21	2.37	0.08	0.27	7.29	73.17
$\widehat{\text{EZ3S}}_{lev}$	0.87	3.09	0.38	1.05	6.97	65.16
$\overline{\text{AA3S}}_{lev}$	-0.10	3.19	0.03	0.05	1.98	9.70

We reproduce the impulse responses plots for the present model with financial leverage. This exercise is the same as the one we have done for the model with exogenous market dividends.

We assume that the economy remains in the second regime for a long time without the impact of innovation shocks. The capital stock and state belief vector stay at their steady-state levels accordingly. In the fifth period, productivity growth shifts from the second regime to the first regime, and following the regime shift, the productivity growth rate evolves according to the three-state MS model. We simulate productivity growth rates from the the three-state MS model after the regime shift, taking into account persistence of regimes characterized by the transition probabilities. We compute macroeconomic quantities and financial variables to investigate impulse responses to changes in state variables. The results shown in Figure 2 are qualitatively similar to those for the model with exogenous market dividends

Figure 1: **Impulse responses**

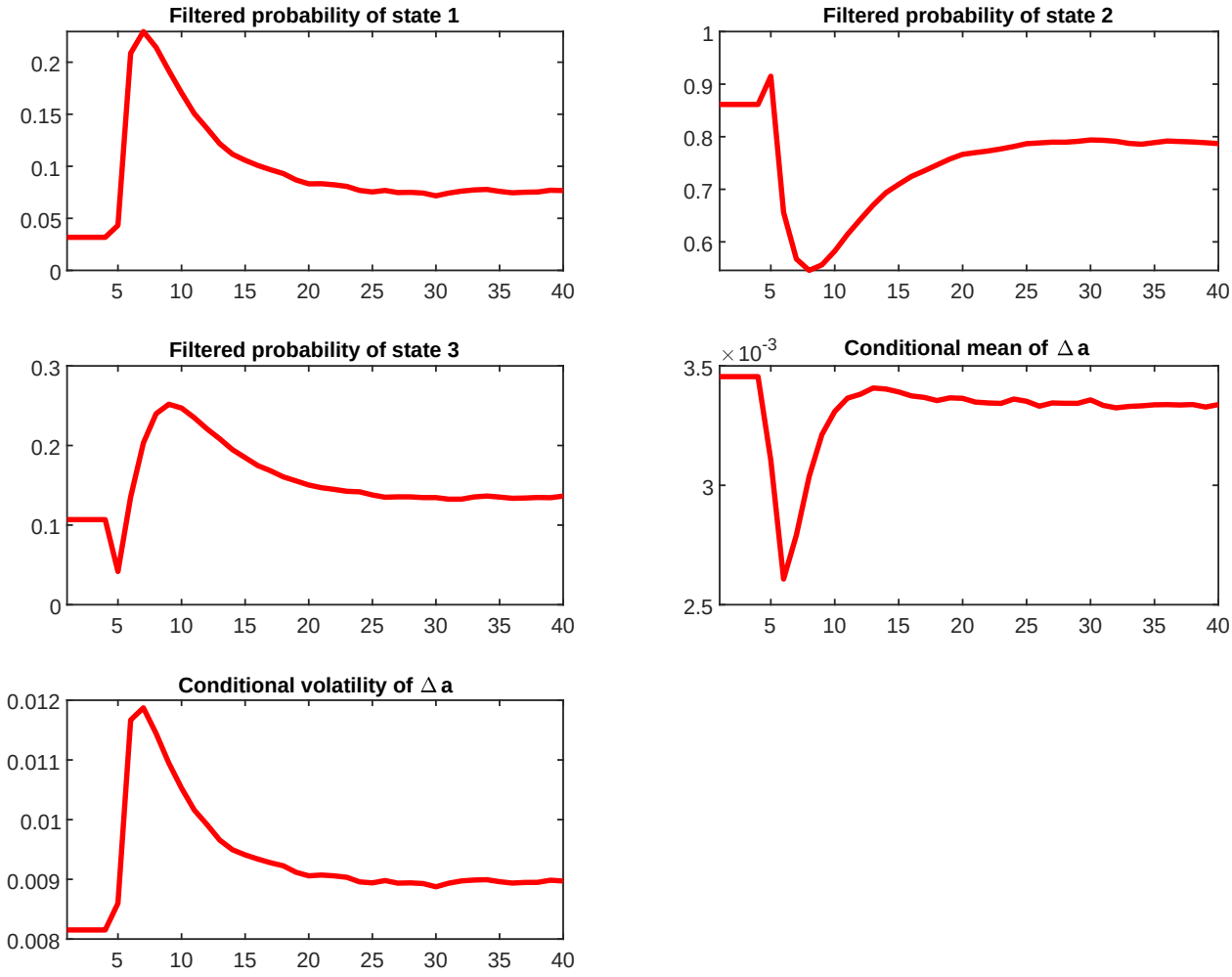

Notes: This figure plots the impulse response functions for the benchmark model AA3S when the economy switches from regime 2 to regime 1. The plots include filtered probabilities of the three states in the MS model and conditional mean and volatility of productivity growth.

Figure 2: **Impulse responses**

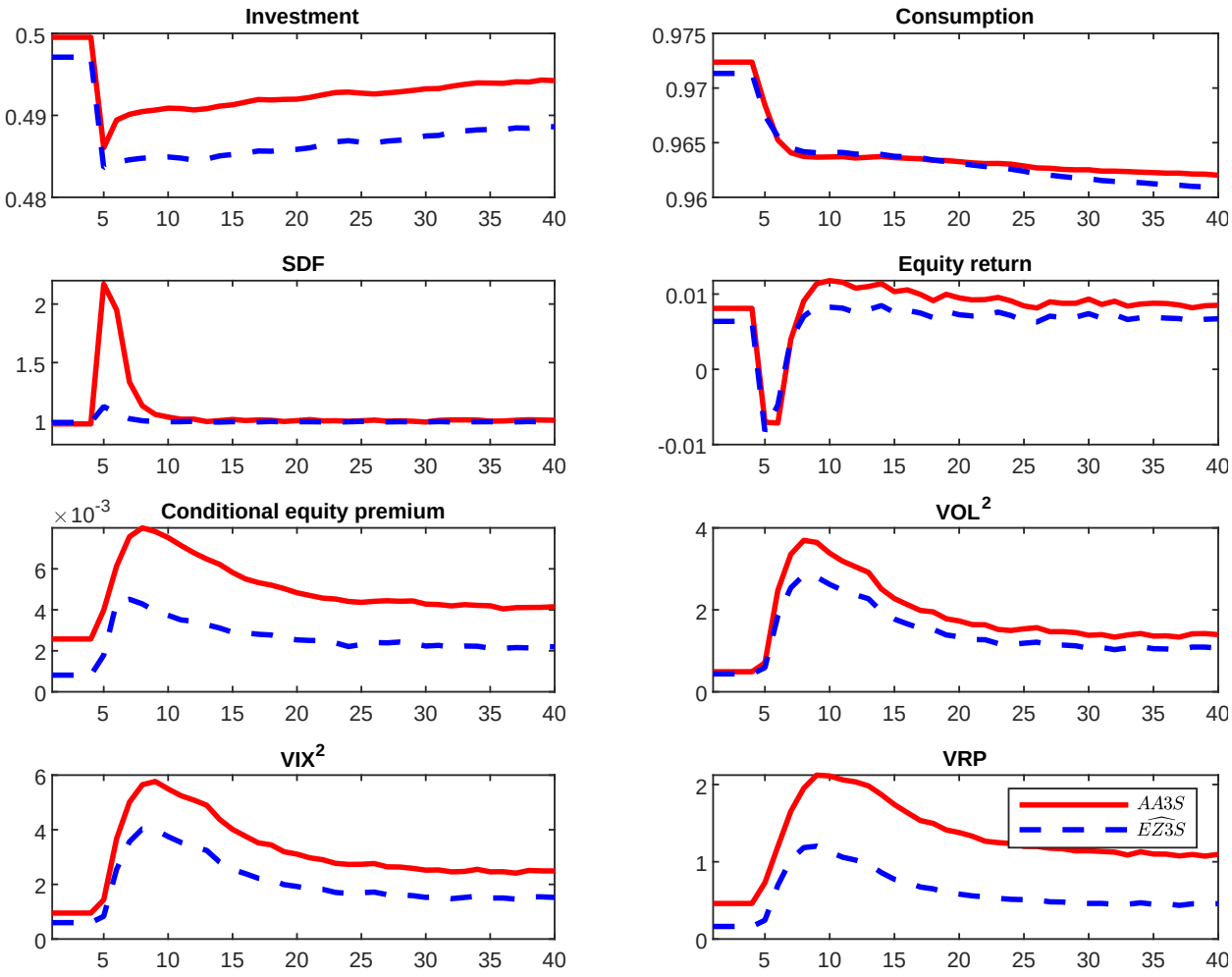

Figure 3: **Cross correlations with quantities and equity return**

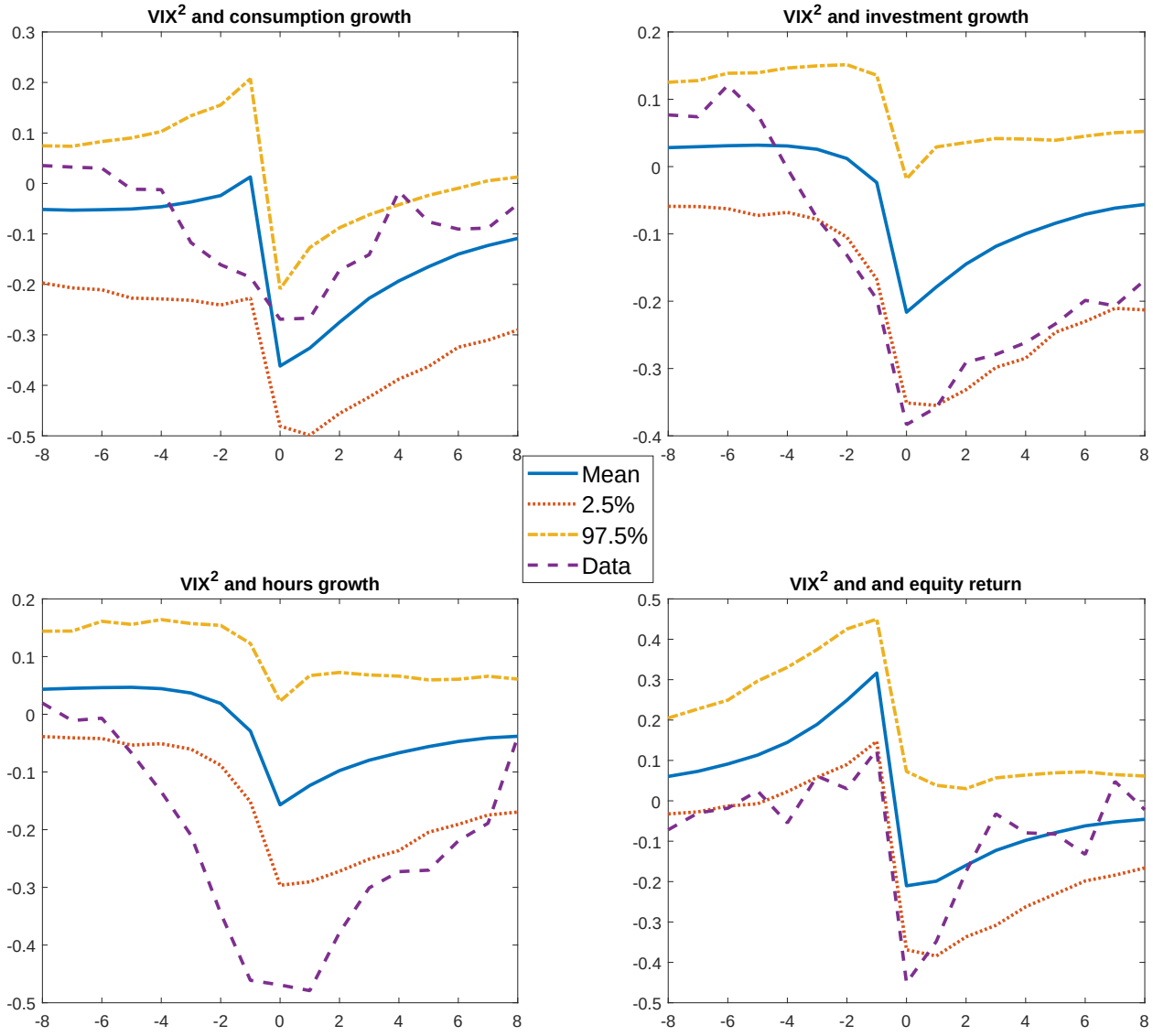

Notes: This figure plots the cross-correlograms between the risk-neutral variance and consumption growth, investment growth, hours growth, and the equity return (i.e., $Corr\left(VIX_t^2, x_{t+k}\right)$ for $k = -8$ to 8). The figure displays correlations for the historical data and the benchmark model AA3S. The cross-correlations are obtained on 2,000 simulated sample paths of the benchmark model. The plots show the mean cross-correlations and the associated 2.5% and 97.5% ranges. The historical data span quarterly data from 1990:Q1 to 2016:Q1.

Figure 4: **Cross correlations with volatilities of quantities and equity return**

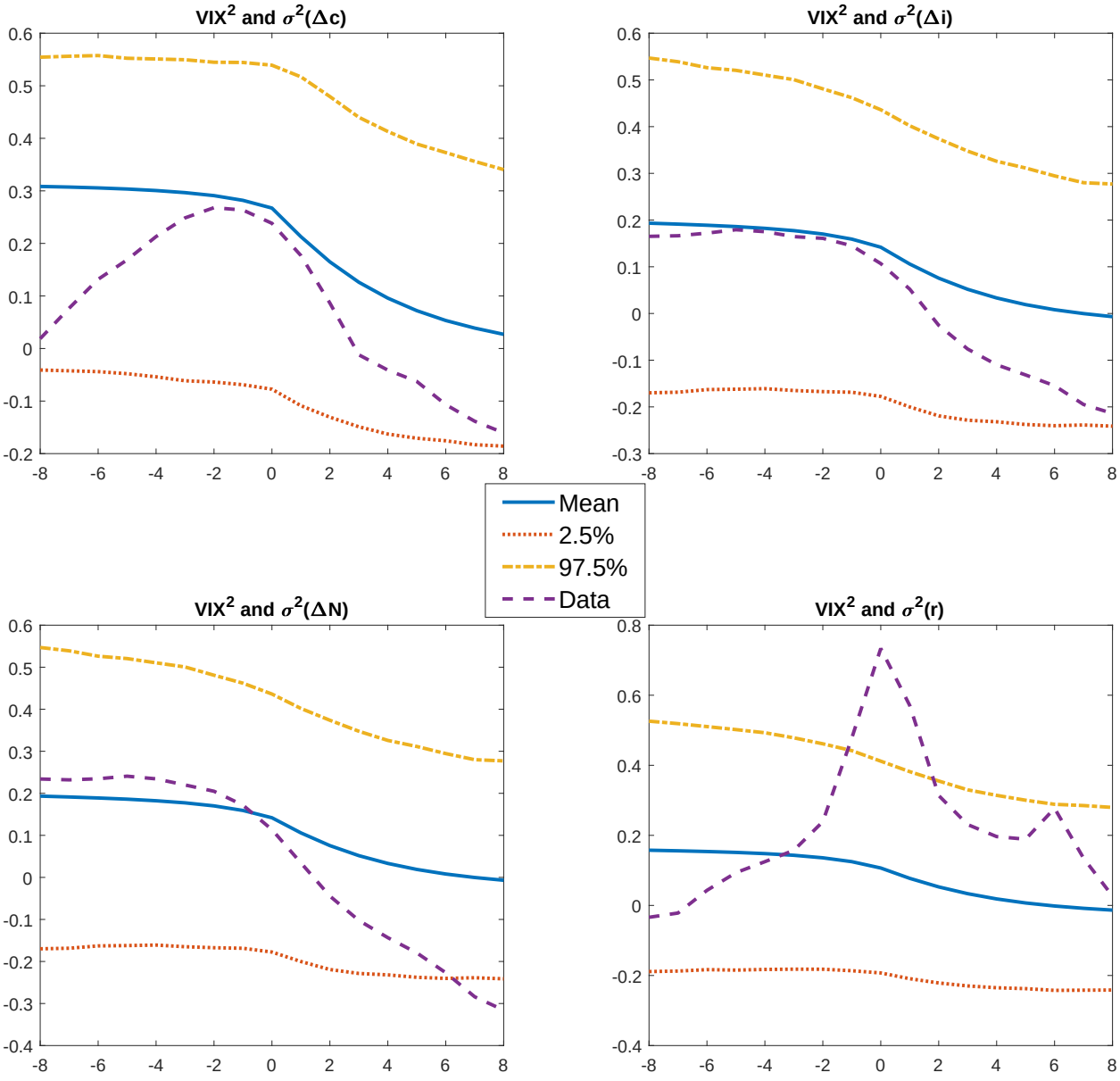

Notes: This figure plots the cross-correlograms between the risk-neutral variance and conditional volatilities of consumption growth, investment growth, and equity returns (i.e., $Corr\left(VIX_t^2, \sigma_{x,t+k}\right)$ for $k = -8$ to 8). The figure displays correlations for the historical data and the benchmark model AA3S. The cross-correlations are obtained on 2,000 simulated sample paths of the benchmark model. The plots show the mean cross-correlations and the associated 2.5% and 97.5% ranges. Historical data span quarterly data from 1990:Q1 to 2016:Q1.

D3: Model generated time series of VRP

We use the historical TFP growth rate to estimate the conditional probabilities of the 3 regimes and then further compute the time series of the model VIX^2 and VRP. The contemporaneous correlation between the model VIX^2 and the historical VIX^2 is about 0.37 ($p = 0.000$). In the contemporaneous regression of the historical VIX^2 on the model VIX^2, the R^2 is 13%. The correlation between our model VRP and historical VRP is 0.18 ($p = 0.062$) and the contemporaneous regression R^2 is 1%. We also construct an alternative VRP measure using our model VIX^2 minus the historical return variance. The correlation between this alternative model VRP and historical VRP is 0.66 ($p = 0.000$) and the contemporaneous regression R^2 is 44%. In Figure 5, we plot the time series of this alternative VRP measure against the historical VRP and the model VIX^2 against the data. Overall, these results suggest that the time variation in conditional mean or volatility of productivity growth can partially explain the variation in the historical VIX^2 and VRP, mostly at the low frequency.

Figure 5: **Model generated time series of VIX^2 and VRP**

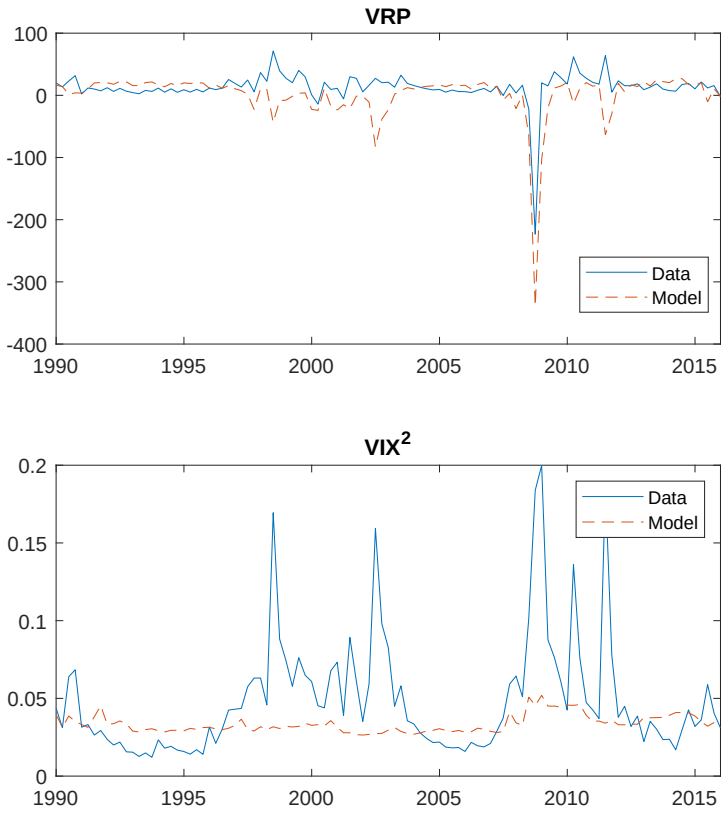

Notes: This figure plots the model generated time series of VIX^2 and VRP against those of the actual data. The model generated time series are computed with the historical TFP growth rate and the probabilities of the 3 states. Historical data span quarterly data from 1990:Q1 to 2016:Q1.

D4: Return predictability

The extant literature finds that the market VRP positively predicts stock returns (Bollerslev et al. (2009), Drechsler and Yaron (2011), Zhou (2018) and Feunou, Jahan-Parvar, and Okou (2018)). These studies find that this predictability is significant at short-to-medium horizons of returns, typically within a year. Table D4 Panel A presents estimation results we obtained by regressing a one

quarter excess return to one-, two-, and three-year cumulative excess returns onto our constructed VRP. The predictability is significant only at the one quarter horizon, with the R^2 being equal to 5.6%. The corresponding slope estimate is positive, indicating that the VRP positively forecasts future returns. We also use the log dividend yield to report the predictive regression results; in so doing, our results are consistent with the extant literature. The dividend yield positively forecasts future returns, and predictability increases in the horizon.

Table D4 also presents the predictability results simulated from models AA3S (Panel B), $\overline{\text{AA3S}}$ (Panel C), EZ3S (Panel D), and AA2S (Panel E). These results are based on averages of 2,000 simulated samples. Both models AA3S and EZ3S reproduce the predictability by the dividend yield that becomes stronger for longer horizons of returns. This model also generates predictability by the VRP: a high current VRP forecasts high future returns. The average R^2 is 2 percent at a one quarter horizon and becomes higher at longer horizons. Hence, both dividend yield and VRP predicts risk premium in our model. However, the extant literature finds that the predictability by the VRP shows a hump-shaped pattern that peaks at a one quarter horizon, a pattern that we cannot replicate in simulations. That said, future research could extend the current model to account for this pattern. In contrast, the $\overline{\text{AA3S}}$ model with constant productivity volatility fails to generate strong predictability by the VRP and the dividend yield at short horizons.

Table D4: **Return Predictability**

		1Q	1Y	2Y	3Y
Panel A: Data					
$\ln(D/P)$	slope	0.047	0.222	0.468	0.729
	R^2	0.033	0.154	0.257	0.310
VRP	slope	0.542	-0.302	-0.854	-0.900
	R^2	0.056	0.004	0.011	0.006
Panel B: Model AA3S					
$\ln(D/P)$	slope	0.1021	0.1890	0.2617	0.3233
	R^2	0.0255	0.0463	0.0626	0.0757
VRP	slope	0.0010	0.0018	0.0024	0.0029
	R^2	0.0205	0.0330	0.0420	0.0490
Panel C: Model $\overline{\text{AA3S}}$					
$\ln(D/P)$	slope	0.0528	0.1014	0.1469	0.1891
	R^2	0.0099	0.0188	0.0269	0.0343
VRP	slope	0.0093	0.0189	0.0289	0.0387
	R^2	0.0080	0.0137	0.0184	0.0223
Panel D: Model EZ3S					
$\ln(D/P)$	slope	0.1097	0.1972	0.2689	0.3291
	R^2	0.0282	0.0492	0.0652	0.0780
VRP	slope	0.0009	0.0017	0.0022	0.0027
	R^2	0.0249	0.0404	0.0507	0.0580

This table reports return predictability results. The dependent variable is the excess equity return $R - R_f$. The two independent variables are the log dividend yield $\ln(D/P)$ and variance risk premium. Univariate predictive regressions are estimated by the OLS method. The horizon of returns ranges from one quarter to three years. The results for models AA3S, $\overline{\text{AA3S}}$ and EZ3S are obtained by averaging over 2,000 simulated samples.

E: Wealth-gamble risk aversion under smooth ambiguity

In this section, we closely follow the approach of Swanson (2012, 2018) to derive wealth-gamble risk aversion measures under smooth ambiguity. Interested readers should refer to Swanson (2018) for a rigorous treatment. We assume that the instantaneous utility function and the value function satisfy regular conditions as in Swanson (2018) (Assumptions 1–7). Due to model uncertainty, there might not exist nonstochastic steady-state, and thus, we will not derive wealth-gamble risk aversion measures at nonstochastic steady-state.

The representative agent's flow budget constraint in each period is

$$x_{t+1} = \left(1 + r_t^K\right) x_t + w_t N_t + F_t - C_t$$

where x_t denotes beginning-of-period assets and w_t, r_t^K, and F_t denote the real wage, real interest rate, and net transfer payments to the agent, respectively. We assume that the agent considers a finite set of stochastic processes $\boldsymbol{\theta}_t$ driving the processes for w_t, r_t^K, and F_t. At each date t, the agent's posterior belief over the set of models is denoted by the vector π_t, which is updated according to Bayes' rule, given some prior π_0. In the agent's optimization problem, the state vector and information set at each date t are collected as $(x_t; \boldsymbol{\theta}_t, \pi_t)$.

We deviate from Swanson (2018) by considering the value function under smooth ambiguity

$$V\left(x_t; \boldsymbol{\theta}_t, \pi_t\right) = \max_{(C_t, N_t)} u\left(C_t, N_t\right) + \beta \left(\sum_j \pi_t\left(j\right) \left(\mathbb{E}_{j,t}\left[V\left(x_{t+1}; \boldsymbol{\theta}_{t+1}, \pi_{t+1}\right)\right]\right)^{1-\eta} \right)^{\frac{1}{1-\eta}} \tag{1}$$

where $j = 1, ..., J$ is an indicator of a model, $\pi_t\left(j\right)$ is the posterior probability of model j at date t, η is the ambiguity aversion parameter satisfying $\eta > 0, \neq 1$. Absent from ambiguity aversion ($\eta = 0$), the utility function (1) reduces to expected utility. This utility function is an extension of the power-power specification of the smooth ambiguity utility function adopted in Ju and Miao (2007) by including the labor margin. We suppress the intertemporal substitution channel to focus on the impact of smooth ambiguity on wealth-gamble risk aversion measures, which does not crucially depend on the intertemporal substitution channel. Incorporating the role of intertemporal substitution will lead to more complicated expressions of wealth-gamble risk aversion measures.

The definition of the coefficient of absolute wealth-gamble risk aversion is given in Definition 1, Swanson (2018). The coefficient of absolute wealth-gamble risk aversion is related to the amount of goods (μ) that the agent is willing to pay to avoid a one-shot gamble of size σ in the flow budget constraint, i.e.,

$$x_{t+1} = \left(1 + r_t^K\right) x_t + w_t N_t + F_t - C_t + \sigma \varepsilon_{t+1}$$

where ε_{t+1} has bounded support, mean zero and unit variance and is independent of other shocks in the model. The one-shot fee μ that the agent would be willing to pay at date t to avoid the gamble appears in the budget constraint

$$x_{t+1} = \left(1 + r_t^K\right) x_t + w_t N_t + F_t - C_t - \mu.$$

We seek the value of μ at $(x_t; \boldsymbol{\theta}_t, \pi_t)$ such that $V\left(x_t - \frac{\mu}{1+r_t^K}; \boldsymbol{\theta}_t, \pi_t\right) = \hat{V}\left(x_t; \boldsymbol{\theta}_t, \pi_t; \sigma\right)$, where $\hat{V}\left(x_t; \boldsymbol{\theta}_t, \pi_t; \sigma\right)$ denotes the value function incorporating the one-shot gamble. The coefficient of absolute wealth-gamble risk aversion is defined to be $R^{a,SA}\left(x_t; \boldsymbol{\theta}_t, \pi_t\right) = \lim_{\sigma \to 0} \mu\left(x_t; \boldsymbol{\theta}_t, \pi_t; \sigma\right) / \left(\sigma^2/2\right)$.

Proposition *Suppose that $(x_t; \boldsymbol{\theta}_t, \pi_t)$ is an interior point of its domain and that the instantaneous utility function and the value function satisfy regular conditions in Swanson (2018). Under the power-power specification of smooth ambiguity preferences given in* (1)*, the agent's coefficient of absolute wealth-gamble risk aversion, $R^{a,SA}\left(a_t, \theta_t\right)$, is given by*

$$R^{a,SA}\left(x_t; \boldsymbol{\theta}_t, \pi_t\right) = \frac{-\sum_j \pi_t\left(j\right) \left(\mathbb{E}_{j,t}\left[V\left(x_{t+1}^*; \boldsymbol{\theta}_{t+1}, \pi_{t+1}\right)\right]\right)^{-\eta} \mathbb{E}_{j,t}\left[V_{11}\left(x_{t+1}^*; \boldsymbol{\theta}_{t+1}, \pi_{t+1}\right)\right]}{\sum_j \pi_t\left(j\right) \left(\mathbb{E}_{j,t}\left[V\left(x_{t+1}^*; \boldsymbol{\theta}_{t+1}, \pi_{t+1}\right)\right]\right)^{-\eta} \mathbb{E}_{j,t}\left[V_1\left(x_{t+1}^*; \boldsymbol{\theta}_{t+1}, \pi_{t+1}\right)\right]}$$

Proof.

The proof builds on the proof of Proposition 1 in Swanson (2018). By the same arguments in Swanson (2018), $\hat{V}\left(x_t; \boldsymbol{\theta}_t, \pi_t; \sigma\right)$ exists, and there exists a unique $-\mu\left(\sigma\right)$ such that $V\left(x_t - \frac{\mu(\sigma)}{1+r_t^K}; \boldsymbol{\theta}_t, \pi_t\right) = \hat{V}\left(x_t; \boldsymbol{\theta}_t, \pi_t; \sigma\right)$

For the recursive smooth ambiguity utility function (1), the first-order conditions for C_t^* and

N_t^* are

$$\begin{aligned} u_1\left(C_t^*, N_t^*\right) &= \beta\left(\sum_j \pi_t(j)\left(\mathbb{E}_{j,t}\left[V\left(x_{t+1}^*;\boldsymbol{\theta}_{t+1},\pi_{t+1}\right)\right]\right)^{1-\eta}\right)^{\frac{\eta}{1-\eta}} \\ &\quad \sum_j \pi_t(j)\left(\mathbb{E}_{j,t}\left[V\left(x_{t+1}^*;\boldsymbol{\theta}_{t+1},\pi_{t+1}\right)\right]\right)^{-\eta}\mathbb{E}_{j,t}\left[V_1\left(x_{t+1}^*;\boldsymbol{\theta}_{t+1},\pi_{t+1}\right)\right] \end{aligned}$$

$$\begin{aligned} u_2\left(C_t^*, N_t^*\right) &= -\beta w_t\left(\sum_j \pi_t(j)\,\mathbb{E}_{j,t}V\left(x_{t+1}^*;\boldsymbol{\theta}_{t+1},\pi_{t+1}\right)^{1-\eta}\right)^{\frac{\eta}{1-\eta}} \\ &\quad \sum_j \pi_t(j)\left(\mathbb{E}_{j,t}\left[V\left(x_{t+1}^*;\boldsymbol{\theta}_{t+1},\pi_{t+1}\right)\right]\right)^{-\eta}\mathbb{E}_{j,t}\left[V_1\left(x_{t+1}^*;\boldsymbol{\theta}_{t+1},\pi_{t+1}\right)\right] \end{aligned}$$

which implies $u_2\left(C_t^*, N_t^*\right) = -w_t u_1\left(C_t^*, N_t^*\right)$.

The first-order effect on the agent's welfare is

$$\begin{aligned} & -V_1\left(x_t;\boldsymbol{\theta}_t,\pi_t\right)\frac{d\mu}{1+r_t^K} \\ = & -\beta\left(\sum_j \pi_t(j)\left(\mathbb{E}_{j,t}\left[V\left(x_{t+1}^*;\boldsymbol{\theta}_{t+1},\pi_{t+1}\right)\right]\right)^{1-\eta}\right)^{\frac{\eta}{1-\eta}} \\ & \cdot\sum_j \pi_t(j)\left(\mathbb{E}_{j,t}\left[V\left(x_{t+1}^*;\boldsymbol{\theta}_{t+1},\pi_{t+1}\right)\right]\right)^{-\eta}\mathbb{E}_{j,t}\left[V_1\left(x_{t+1}^*;\boldsymbol{\theta}_{t+1},\pi_{t+1}\right)\right]d\mu \end{aligned} \tag{2}$$

Differentiating (1) with respect to a_t yields

$$\begin{aligned} V_1\left(x_t;\boldsymbol{\theta}_t,\pi_t\right) &= u_1\left(C_t^*, N_t^*\right)\frac{\partial C_t^*}{\partial a_t} + u_2\left(C_t^*, N_t^*\right)\frac{\partial N_t^*}{\partial a_t} + \beta\left(\sum_j \pi_t(j)\left(\mathbb{E}_{j,t}\left[V\left(x_{t+1}^*;\boldsymbol{\theta}_{t+1},\pi_{t+1}\right)\right]\right)^{1-\eta}\right)^{\frac{\eta}{1-\eta}} \\ & \cdot\sum_j \pi_t(j)\left(\mathbb{E}_{j,t}\left[V\left(x_{t+1}^*;\boldsymbol{\theta}_{t+1},\pi_{t+1}\right)\right]\right)^{-\eta}\mathbb{E}_{j,t}\left[V_1\left(V\left(x_{t+1}^*;\boldsymbol{\theta}_{t+1},\pi_{t+1}\right)\right)\right] \\ & \cdot\left[1+r_t^K - \frac{\partial C_t^*}{\partial a_t} + w_t\frac{\partial N_t^*}{\partial a_t}\right] \end{aligned}$$

Substituting $u_1\left(C_t^*, N_t^*\right)$ and $u_2\left(C_t^*, N_t^*\right)$ into the equation above yields the envelop theorem:

$$\begin{aligned} V_1\left(x_t; \boldsymbol{\theta}_t, \pi_t\right) &= \beta\left(1+r_t^K\right)\left(\sum_j \pi_t\left(j\right)\left(\mathbb{E}_{j,t}\left[V\left(x_{t+1}^*; \boldsymbol{\theta}_{t+1}, \pi_{t+1}\right)\right]\right)^{1-\eta}\right)^{\frac{\eta}{1-\eta}} \\ &\quad \cdot \sum_j \pi_t\left(j\right)\left(\mathbb{E}_{j,t}\left[V\left(x_{t+1}^*; \boldsymbol{\theta}_{t+1}, \pi_{t+1}\right)\right]\right)^{-\eta} \mathbb{E}_{j,t}\left[V_1\left(x_{t+1}^*; \boldsymbol{\theta}_{t+1}, \pi_{t+1}\right)\right] \end{aligned}$$

and the Benveniste–Scheinkman equation

$$V_1\left(x_t; \boldsymbol{\theta}_t, \pi_t\right) = \left(1+r_t^K\right) u_1\left(C_t^*, N_t^*\right)$$

The agent's value function, inclusive of the one-shot gamble satisfies

$$\hat{V}\left(x_t; \boldsymbol{\theta}_t, \pi_t; \sigma\right) = u\left(C_t^*, N_t^*\right) + \beta\left(\sum_j \pi_t\left(j\right)\left(\mathbb{E}_{j,t}\left[V\left(x_{t+1}^*; \boldsymbol{\theta}_{t+1}, \pi_{t+1}\right)\right]\right)^{1-\eta}\right)^{\frac{1}{1-\eta}} \tag{3}$$

Differentiating (3) with respect to σ, we obtain the first-order effect of the gamble on the agent's welfare

$$\begin{aligned} &\left[u_1 \frac{\partial C_t^*}{\partial \sigma} + u_2 \frac{\partial N_t^*}{\partial \sigma} + \beta\left(\sum_j \pi_t\left(j\right)\left(\mathbb{E}_{j,t}\left[V\right]\right)^{1-\eta}\right)^{\frac{\eta}{1-\eta}}\right. \\ &\left. \cdot \sum_j \pi_t\left(j\right)\left(\mathbb{E}_{j,t}\left[V\right]\right)^{-\eta} \mathbb{E}_{j,t}\left[V_1\left(w_t \frac{\partial N_t^*}{\partial \sigma} - \frac{\partial C_t^*}{\partial \sigma} + \varepsilon_{t+1}\right)\right]\right] d\sigma \end{aligned}$$

where the arguments of u_1, u_2, V, and V_1 are suppressed. According to the arguments in Swanson (2018), the first-order effect is zero.

The second-order effect of the gamble is

$$\begin{aligned}
&\Bigg\{ u_{11}\left(\frac{\partial C_t^*}{\partial \sigma}\right)^2 + 2u_{12}\frac{\partial C_t^*}{\partial \sigma}\frac{\partial N_t^*}{\partial \sigma} + u_{22}\left(\frac{\partial N_t^*}{\partial \sigma}\right)^2 + u_1\frac{\partial^2 C_t^*}{\partial \sigma^2} + u_2\frac{\partial^2 N_t^*}{\partial \sigma^2} \\
&+\beta\eta\left(\sum_j \pi_t(j)\left(\mathbb{E}_{j,t}[V]\right)^{1-\eta}\right)^{\frac{2\eta-1}{1-\eta}}\left(\sum_j \pi_t(j)\left(\mathbb{E}_{j,t}[V]\right)^{-\eta}\mathbb{E}_{j,t}\left[V_1\left(w_t\frac{\partial N_t^*}{\partial \sigma} - \frac{\partial C_t^*}{\partial \sigma} + \varepsilon_{t+1}\right)\right]\right)^2 \\
&-\beta\eta\left(\sum_j \pi_t(j)\left(\mathbb{E}_{j,t}[V]\right)^{1-\eta}\right)^{\frac{\eta}{1-\eta}}\sum_j \pi_t(j)\left(\mathbb{E}_{j,t}[V]\right)^{-\eta-1}\left(\mathbb{E}_{j,t}\left[V_1\left(w_t\frac{\partial N_t^*}{\partial \sigma} - \frac{\partial C_t^*}{\partial \sigma} + \varepsilon_{t+1}\right)\right]\right)^2 \\
&+\beta\left(\sum_j \pi_t(j)\left(\mathbb{E}_{j,t}[V]\right)^{1-\eta}\right)^{\frac{\eta}{1-\eta}}\sum_j \pi_t(j)\left(\mathbb{E}_{j,t}[V]\right)^{-\eta}\mathbb{E}_{j,t}\left[V_{11}\left(w_t\frac{\partial N_t^*}{\partial \sigma} - \frac{\partial C_t^*}{\partial \sigma} + \varepsilon_{t+1}\right)^2\right] \\
&+\beta\left(\sum_j \pi_t(j)\left(\mathbb{E}_{j,t}[V]\right)^{1-\eta}\right)^{\frac{\eta}{1-\eta}}\sum_j \pi_t(j)\left(\mathbb{E}_{j,t}[V]\right)^{-\eta}\mathbb{E}_{j,t}\left[V_1\left(w_t\frac{\partial^2 l_t^*}{\partial \sigma^2} - \frac{\partial^2 c_t^*}{\partial \sigma^2}\right)\right]\Bigg\}\frac{d\sigma^2}{2}
\end{aligned}$$

which reduces to

$$\beta\left(\sum_j \pi_t(j)\left(\mathbb{E}_{j,t}[V]\right)^{1-\eta}\right)^{\frac{\eta}{1-\eta}}\left(\sum_j \pi_t(j)\left(\mathbb{E}_{j,t}[V]\right)^{-\eta}\mathbb{E}_{j,t}[V_{11}]\right)\frac{d\sigma^2}{2} \tag{4}$$

because $\frac{\partial C_t^*}{\partial \sigma}$, $\frac{\partial N_t^*}{\partial \sigma}$, $\frac{\partial^2 C_t^*}{\partial \sigma^2}$, and $\frac{\partial^2 N_t^*}{\partial \sigma^2}$ are all zeros and ε_{t+1} is independent of other shocks.

Given that Eq. (2) and Eq. (4) are equal, the definition of the coefficient of wealth-gamble risk aversion implies

$$R_t^{a,SA} = \frac{-\sum_j \pi_t(j)\left(\mathbb{E}_{j,t}[V]\right)^{-\eta}\mathbb{E}_{j,t}[V_{11}]}{\sum_j \pi_t(j)\left(\mathbb{E}_{j,t}[V]\right)^{-\eta}\mathbb{E}_{j,t}[V_1]} \qquad \textbf{Q.E.D.}$$

Regarding the derivatives of the value function V_1 and V_{11}, the following results hold. The Benveniste–Scheinkman equation still holds under smooth ambiguity:

$$V_1(x_t;\boldsymbol{\theta}_t,\pi_t) = \left(1+r_t^K\right)u_1\left(C_t^*,N_t^*\right)$$

Further differentiating the Benveniste–Scheinkman equation with respect to x_t yields

$$V_{11}(x_t;\boldsymbol{\theta}_t,\pi_t) = \left(1+r_t^K\right)\left[u_{11}\left(C_t^*,N_t^*\right)\frac{\partial C_t^*}{\partial a_t} + u_{12}\left(C_t^*,N_t^*\right)\frac{\partial N_t^*}{\partial a_t}\right]$$

Additionally, differentiating the intratemporal optimality condition with respect to x_t yields

$$\frac{\partial N_t^*}{\partial a_t} = -\lambda_t \frac{\partial C_t^*}{\partial a_t}$$

where λ_t is given by

$$\lambda_t = \frac{u_1\left(C_t^*, N_t^*\right) u_{12}\left(C_t^*, N_t^*\right) - u_2\left(C_t^*, N_t^*\right) u_{11}\left(C_t^*, N_t^*\right)}{u_1\left(C_t^*, N_t^*\right) u_{22}\left(C_t^*, N_t^*\right) - u_2\left(C_t^*, N_t^*\right) u_{12}\left(C_t^*, N_t^*\right)}$$

Using the utility gradient approach as in Ju and Miao (2007), we obtain the stochastic discount factor for the recursive smooth ambiguity utility function (1)

$$m_{t+1} = \beta \frac{u_1\left(C_{t+1}^*, N_{t+1}^*\right)}{u_1\left(C_t^*, N_t^*\right)} \frac{\left(\mathbb{E}_{j,t}\left[V\left(x_{t+1}^*; \boldsymbol{\theta}_{t+1}, \pi_{t+1}\right)\right]\right)^{-\eta}}{\left(\sum_j \pi_t(j)\left[\left(\mathbb{E}_{j,t}\left[V\left(x_{t+1}^*; \boldsymbol{\theta}_{t+1}, \pi_{t+1}\right)\right]\right)^{1-\eta}\right]\right)^{\frac{-\eta}{1-\eta}}}$$

According to Definition 2 and Definition 3 in Swanson (2018), the consumption-wealth coefficient of relative wealth-gamble risk aversion and the consumption-and-leisure-wealth coefficient of relative wealth-gamble risk aversion, respectively, are given by

$$\begin{aligned} R_t^{c,SA}\left(x_t; \boldsymbol{\theta}_t, \pi_t\right) &= Z_t^C R_t^{a,SA}\left(x_t; \boldsymbol{\theta}_t, \pi_t\right) \\ R_t^{c,SA}\left(x_t; \boldsymbol{\theta}_t, \pi_t\right) &= Z_t^{CN} R_t^{a,SA}\left(x_t; \boldsymbol{\theta}_t, \pi_t\right) \end{aligned}$$

where

$$\begin{aligned} Z_t^C &= \left(1 + r_t^K\right)^{-1} E_t\left[\sum_{\tau=t}^{\infty} m_{t,\tau} C_\tau^*\right] \\ Z_t^C &= \left(1 + r_t^K\right)^{-1} E_t\left[\sum_{\tau=t}^{\infty} m_{t,\tau}\left(C_\tau^* + w_\tau\left(\bar{N} - N_\tau^*\right)\right)\right] \end{aligned}$$

in which $m_{t,\tau} = \prod_{s=t}^{\tau-1} m_{s+1}$ is the multiperiod stochastic discount factor.

References

Anderson, E. W., Hansen, L. P., Sargent, T. J., 2003. A quartet of semigroups for model specification, robustness, price of risk, and model detection. Journal of the European Economic Association 1, 68–123.

Bollerslev, T., Tauchen, G., Zhou, H., 2009. Expected stock returns and variance risk premia. Review of Financial Studies 22, 4463–4492.

Camerer, C. F., 1999. Uncertain Decisions: Bridging Theory and Experiments. Kluwer Academic Publishers, Ch. Ambiguity Aversion and Non-Additive Probability: Experimental Evidence, Models and Applications, pp. 53–80.

Drechsler, I., Yaron, A., 2011. What's vol got to do with it. Review of Financial Studies 24, 1–45.

Feunou, B., Jahan-Parvar, M. R., Okou, C., 2018. Downside variance risk premium. Journal of Financial Econometrics 16, 341–383.

Halevy, Y., 2007. Ellsberg revisited: An experimental study. Econometrica 75, 503–536.

Ju, N., Miao, J., 2007. Ambiguity, learning, and asset returns. Working paper.

Ju, N., Miao, J., 2012. Ambiguity, learning, and asset returns. Econometrica 80, 559–591.

Stock, J., Watson, M., 1999. Business cycle fluctuations in us macroeconomic time series. In: J. Taylor and M. Woodford (eds.), *Handbook of Macroeconomics*, Amsterdam, Elsevier.

Swanson, E. T., 2012. Risk aversion and the labor margin in dynamic equilibrium models. American Economic Review 102, 1663–1691.

Swanson, E. T., 2018. Risk aversion, risk premia, and the labor margin with generalized recursive preferences. Review of Economic Dynamics 28, 290–321.

Zhou, H., 2018. Variance risk premia, asset predictability puzzles, and macroeconomic uncertainty. Annual Review of Financial Economics 10, 481–497.